High-speed Video Observation and On-line Measurements of Oil Aeration in an Internal Combustion Engine

by

Devon L. Manz

B.E., Mechanical Engineering
University of Saskatchewan, 2003

Submitted to the Department of Mechanical Engineering in Partial Fulfillment of the Requirements for the Degree of

MASTER OF SCIENCE IN MECHANICAL ENGINEERING
AT THE
MASSACHUSETTS INSTITUTE OF TECHNOLOGY

JUNE 2005

Signature of Author: _____
Department of Mechanical Engineering
May 6, 2005

Certified by: _____
Wai K. Cheng
Professor of Mechanical Engineering
Thesis Supervisor

Accepted by: _____
Lallit Anand
Chairman, Departmental Graduate Committee

(This page is intentionally blank)

High-speed Video Observation and On-line Measurements of Oil Aeration in an Internal Combustion Engine

by
Devon L. Manz

B.E., Mechanical Engineering
University of Saskatchewan, 2003

ABSTRACT

Along the oil's journey through the oil lube system, the oil lubricates, cools, removes impurities, supports load, and minimizes friction. At the end of the oil's journey it returns to the sump where it remains nearly motionless until it re-enters the oil pick-up and restarts its journey. This study is focused on the creation and destruction mechanisms of air in the oil. To study this, a motored Ford 3.0L V6 DOHC engine test apparatus was designed, fabricated and instrumented to operate at 8000rpm and at engine oil temperatures below 110°C. Visual observations and quantitative measurements of oil aeration were performed in the oil sump.

The oil aeration process was visualized in the oil sump using high-speed video equipment, at engine speeds below 4000rpm. Oil droplets were observed to depart the crankshaft at approximately the tangential velocity, pass through drainage gaps in the windage tray, and strike the free surface of the oil. The rhythmic pulsation of oil droplets on the free surface caused the surface to slosh at the frequency of the crankshaft's rotation. Foam was observed to form above a threshold speed and a threshold temperature. The windage tray was observed to reduce the droplet number density. When the windage tray was removed, the increased droplet number density inhibited foam formation.

An x-ray absorption measurement technique was used to measure oil aeration at multiple locations in the oil sump. An experimental methodology was developed and preliminary experiments were performed with and without the windage tray at oil volumes below 5L, engine speeds below 6000rpm, and oil temperatures below 110°C. Aeration measurements reveal a general increase in aeration as a function of engine speed at all locations in the oil sump.

In the oil sump, more air is present at the oil surface than at the oil pick-up because air continuously leaves the oil at the air-oil interface. When the engine shuts down, all of the oil in the lube path drains back into the oil sump, and in a short period of time all of the air bubbles rise to the surface and escape the oil. It is the balance between air entering the oil (creation mechanisms) and air leaving the oil (destruction mechanisms) that is the focus of this study.

Thesis Supervisor: Wai Cheng
Title: Professor of Mechanical Engineering

(This page is intentionally blank)

Acknowledgements

Being at MIT has allowed me to realize what I value most, and that has made my time here more valuable than I ever could have imagined. Developing lasting friendships and having the opportunity to study here are gifts that I will cherish for the rest of my life.

Applying my technical skills to the development of a scientific experiment was what I gained most from this project, however Wai Cheng taught me how to conduct scientific research and helped me develop the ability to critically judge experimental results. I would like to thank him for trusting and empowering me with this project. I would also like to thank him for giving me the opportunity to attend conferences, author a paper, perform research on-site at Ford, and present my research at technical meetings and conferences. His trust and supervision permitted me to manage my time according to my schedule, and for that I am grateful.

Jim Cowart is one of the most friendly and enjoyable people that I have ever had the pleasure to work with. Jim was on the research staff in the Sloan Lab and has always been a wonderful resource. His contributions to the development of the apparatus were extremely valuable. During times of uncertainty you can always count on Jim to put everything into perspective.

Thane Dewitt's experience, generosity, dedication, and professionalism has been paramount to the development of my unique and challenging experimental set-up, and I would like to thank him for everything he has done. I would also like to thank Raymond Phan for his dedication and hard work. I could always count on Raymond and Thane for anything and everything I needed.

This project was made possible by the technical and financial support from Feng Shen, Mikhail Ejakov, Ben Ni, and John Pieprzak of Ford POEE. I would like to thank the Natural Sciences and Engineering Research Council of Canada (NSERC) for awarding me the Julie Payette Fellowship. One of the research opportunities made possible by the contributions of Ford and NSERC was the purchase of Air-x, an aeration measurement device developed by Benoit Deconninck and Thierry Delvigne from DSI Deltabeam. I would like to thank Ken Oxorn of ANS Technologies for his Air-x technical support. I would also like to thank Bob Finchum and Bill Hall from the Ramsey Products Corporation for donating the silent chain drive. Brian Palacios from Roush Industries made experiments on a firing engine possible and I would like to thank him for his contributions.

Throughout my coursework and research, Jeff Jocsak has been an excellent resource. His attention to detail and general sharpness gave me the opportunity to think creatively, so thank-you Jeff. My family has provided me with more support and encouragement than anyone could ever wish for. Thank you Jared, Lindsay, Mom, and Dad.

(This page is intentionally blank)

Table of Contents

List of Tables

List of Figures

Chapter 1: Introduction and Background

Engine oil serves multiple functions within an engine, from lubricating and cooling to acting as the working fluid in hydraulic systems. The presence of air in the lubricating oil, termed oil aeration, can be detrimental to many of these functions and it is the aeration process that is the focus of this study.

1.1 Engine Lubrication System

The lubrication system serves multiple functions in an internal combustion engine. The lubricant reduces frictional resistance, protects the engine against wear, contributes to the cooling of engine parts, removes impurities from lubricated regions, and holds gas and oil leakage at an acceptable level [1].

A diagram of the 3.0L DOHC Ford *Duratec* engine lube system is shown in Figure 1-1. Engine oil is collected in the oil sump at near atmospheric pressure. Oil is drawn into the oil pick-up and forced through a screen by the oil pump. The oil flows into the oil filter at the pump pressure and enters the oil main gallery. From the gallery, the oil is fed into the main bearings through four separate oil holes along the gallery. From the main bearings oil is supplied to the connecting rod bearings through the oil bores in the crankshaft. The left cylinder head is supplied with oil from the front of the gallery, while the right cylinder head is supplied oil from the rear of the gallery. The oil in the heads feed each cam bearing and hydraulic lash adjuster. An oil flow restrictor, located between the block and the head, restricts flow and causes the pressure to drop upon entering the heads. From the heads, the oil drains back into the sump through the oil return lines. In addition, oil is also supplied to the timing chain tensioner assembly. The oil flow path is shown in Figure 1-1.

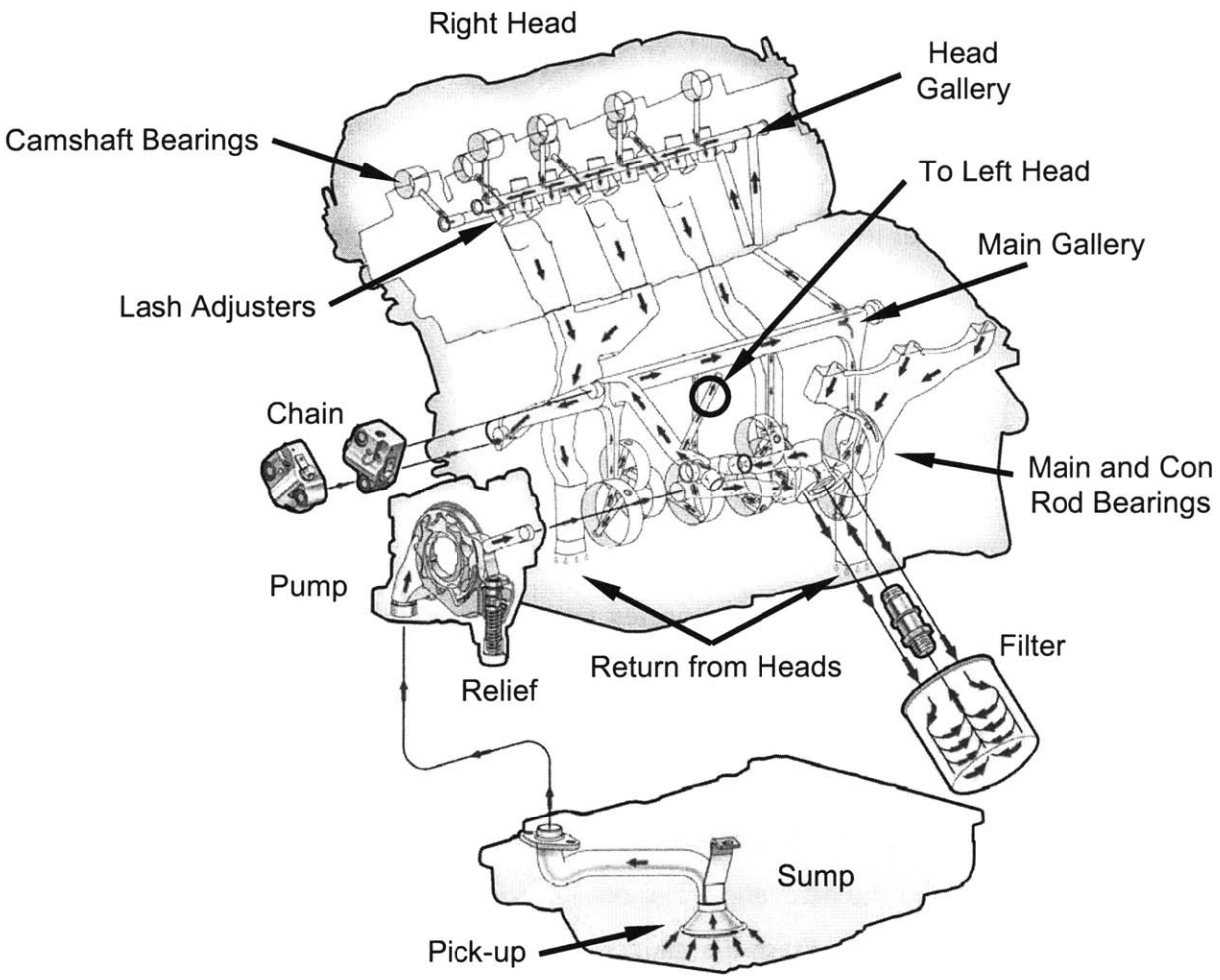

Figure 1-1. 2003 3.0L DOHC Ford *Duratec* engine lubrication system

According to [2], below 3000rpm the oil flow entering the pick-up increases approximately linearly with the engine speed. At approximately 3000rpm, the pump relief valve opens, and the oil flowrate through the lube system remains roughly constant with engine speed. These values were determined for a firing engine at a firing engine oil temperature (140°C at 6000rpm). The total oil flowrate entering the oil-pickup is calculated as the summation of the oil flow into the right and left heads and the oil flow through the block (main and connecting rod bearings). Less oil lubricates the timing chains (assumed to be approximately 50% the value of either of the head flows). The breakdown of the oil flow to the heads, main and connecting rod bearings, and chains is roughly estimated in Figure 1-2. Note that this figure assumes that the pump volumetric efficiency is independent of engine speed (i.e. the flow through the relief valve increases linearly beyond 3000rpm). It should also be noted that this figure has not been

experimentally determined and should only serve as a general trend to explain the oil flowing back into the sump. This information was also used to predict the time to completely turn over the oil in the sump (oil sump resident time).

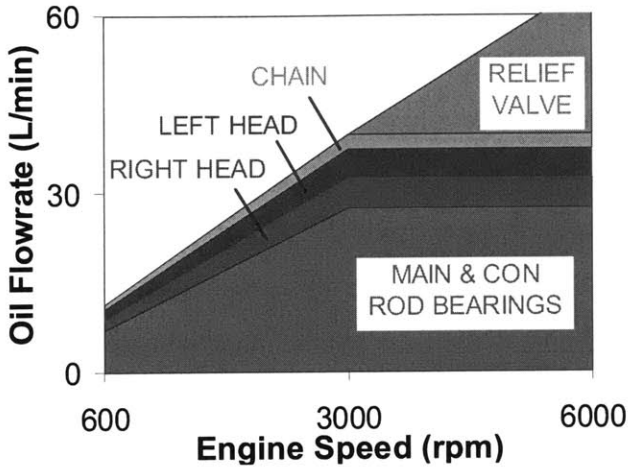

Figure 1-2. Engine oil flow through the various passages in the lube system

After flowing through the lube system, the oil returns to the sump as shown in Figure 1-3.

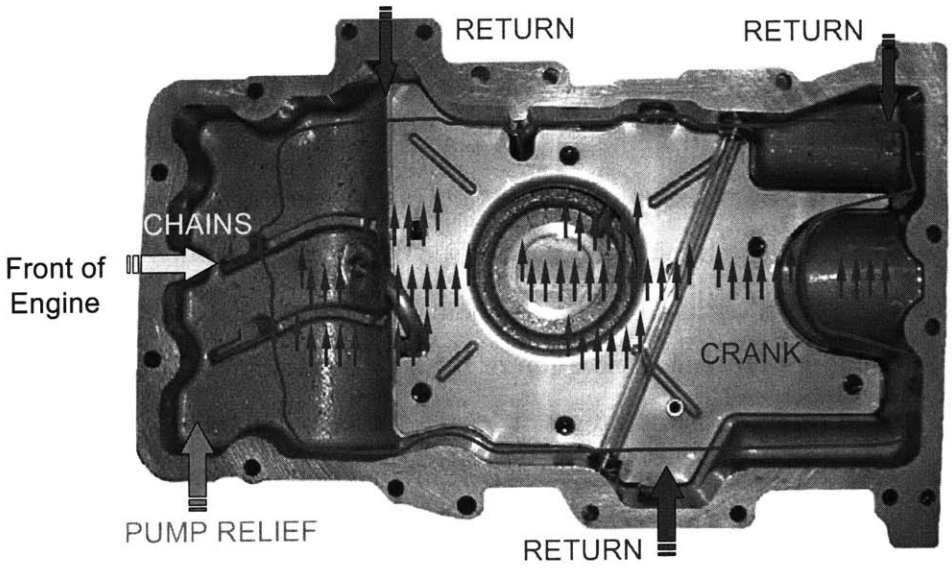

Figure 1-3. Schematic of oil flow into the sump: *Return* – Oil returning from the right head (two entry points) and left head (one entry point), *Crank* – Oil from the connecting rod and main bearings enter the sump as droplets flung from the crankshaft and oil that drains into the sump, *Chains* – Oil from the timing chains, and *Pump Relief* – Oil from the pump, once the relief valve opens.

The Return oil comes from the right head (at two locations) and left head (at one location). The left and right timing chains are driven by the crankshaft and return oil to the sump at the front of the oil pan. Each of the four main bearings is fed from the gallery (see Figure 1-1). The main bearings feed the connecting rod bearings. The oil returns to the sump from the bearings as droplets being flung from the crankshaft into the sump, and as oil draining back into the sump. Once the gallery pressure exceeds a determined pressure, the oil flows back into the sump via the pump relief valve. After returning to the oil sump, the oil from each of sources mix and enter the pick-up situated near the bottom of the oil pan.

Based on experiments with the Ford *Duratec* engine, approximately 2.2L remain in the oil sump during engine operation with 4L of oil. This indicates that the remaining 1.8L of oil must be in transit throughout the rest of the oil lube system. From visual observation, the volume of oil in the sump remained constant between 800rpm and 3000rpm.

1.2 Oil Aeration

1.2.1 Description of Oil Aeration

Lubricating oil systems contain air in the form of bound air and unbound air. Bound air consists of *dissolved air* (air in the oil solution), *entrained air* (air bubbles dispersed through the bulk of the oil) and *foam* (layers of air bubbles on the surface of the oil, separated by thin liquid films, which prevent bubbles from coalescing [3]). Unbound air is separated from the oil. It may be transformed into bound air through dissolution or through entrainment. Dissolved air generally does not cause operational problems unless it leaves the oil solution. This occurs when the temperature increases or pressure decreases [4]. Entrained air results from the dissolved air separating from the oil (changes in ambient conditions) or from unbound air entering the oil (via surface wave entrainment or droplet impingement). Foam results from entrained air bubbles rising above the surface of the oil. These forms of air-oil interaction are shown schematically in Figure 1-4.

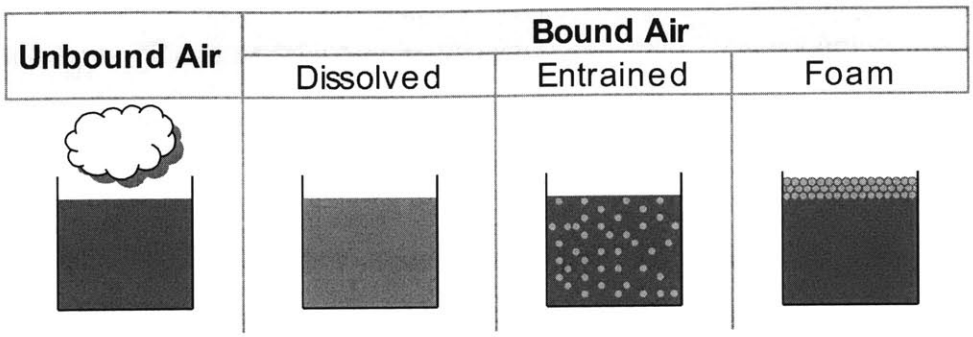

Figure 1-4. Schematic of air-oil mixtures

1.2.2 Causes of Oil Aeration

In addition to the oil properties and composition, the degree of oil aeration depends on several oil and engine parameters such as: Engine speed, oil mass, oil level, oil pan design, oil drain back design, the covering of rotating components, ventilation system design, and blow-back system design [5]. A schematic of parameters that affect oil aeration is shown Figure 1-5.

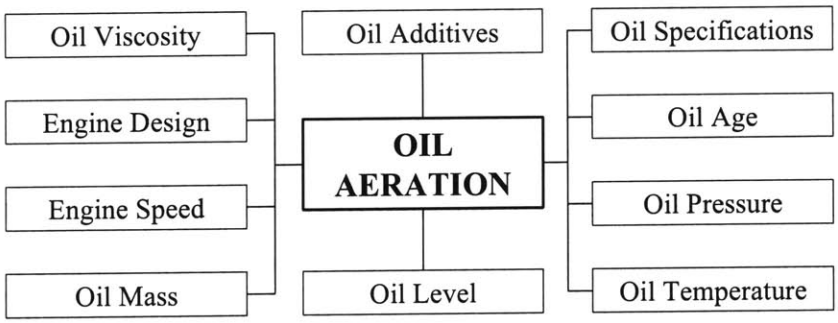

Figure 1-5. The parameters affecting oil aeration

1.2.2.1 Engine Speed

As the engine speed increases the level of oil aeration increases due to faster oil circulation, which decreases the probability that air will escape the oil while in the oil sump (bound air transforming to unbound air) [6]. Conversely, the oil sump foam height has been observed to increase as the engine speed decreases. This suggests that a mechanism exists that inhibits foam growth. According to [7], at high speed and high temperature operating conditions (4000rpm),

the foam height was significantly lower than that observed at the low speed and low temperature operating conditions (2000rpm). The number density of entrained air bubbles tended to increase with engine speed [7].

1.2.2.2 Oil Level

Air may become entrained as a result of increased agitation or splashing in the oil pan. Although this tends to occur at higher engine speeds, reduced oil levels can result in the oil pump drawing in air. Oil may be drawn into the pump during a vehicle maneuver when the oil surface moves below the pick-up. When the oil level is too high, the surface may come into contact with the crankshaft. This will increase the load on the crankshaft and may aerate the oil. However, a higher oil level tends to increase the time required for oil turnover (decrease in oil resident time), which in turn, increases the amount of time available for air to escape the oil in the sump [6].

The oil resident time is the length of time required to completely turn over the oil in the sump. If the oil volume is large enough to permit some air bubbles to leave the oil before it completely turns over, the aeration level has been observed to decrease [5]. Experiments have shown that deeper oil pans result in lower aeration rates; however packaging restraints have limited these designs [5].

1.2.2.3 Component Design

The design of the baffle, windage tray and oil pan is critical to controlling aeration. Funneling of oil in the sump (i.e. the depression of the oil free-surface produced by the pump action) may lead to air entering the oil pump, however baffeling tends to reduce the funneling effect [6]. The separation distance between the oil pump inlet and the bottom of the oil pan may also influence aeration.

When the oil pump flow decreases, as a result of variation in the pressure and flow demands of the system, a corresponding decrease in the oil turnover rate is observed. Reducing the bearing clearance in the main, connecting rod, and camshaft bearings can lead to an improvement in oil foaming behavior because of the reduced oil flow rate. One of the most important measures to reduce the oil foaming is the creation of a suitable oil return system. The target is to lead the oil from the cylinder head directly into the oil pan. If the oil return channels end above the

crankshaft level, there is an increased risk that the oil may contact and become aerated by the crankshaft. However, since the *Duratec* head return lines are separate from the crankshaft, this is not an issue for this engine.

1.2.2.4 Rotating Components

The crankshaft is often considered the primary mechanical contributor to foam formation. As the oil comes into contact with the crankshaft, droplets of oil are flung from the crankshaft and impinge on the surface of the oil. With rotating engine parts churning the oil, the engine's effective output may be reduced by up to 8% [8]. If rotating components are in the vicinity of the oil surface, foaming will raise the oil surface into contact with the rotating components. Examples are: Oil pump driving chains or balancer transmissions. Large quantities of gas bubbles enter the oil via the alternating movement of rotating components [5]. A sufficient covering of these components, especially in direct proximity of the oil suction system, will reduce air entrainment.

1.2.2.5 Oil Composition

Oil formulation influences the number of entrained air bubbles in the oil at high speed and high temperature operating conditions [7]. Temperature, viscosity, degree of refinement, and average molecular weight influence the air solubility, however for commercial engine lubricating oils in the lube system, the effects of these secondary parameters are small relative to the effect of pressure [9]. Aeration and foaming has been observed from fluid contamination due to surface-active compounds or precipitation of air release agents [3]. Blow by gases, wear particles, sediment, and anti-foam agents may influence foaming and aeration levels, however the degree of their influence has not been examined.

1.2.2.6 Engine Load

Compared to engine speed, engine load and oil temperature have less influence on foam formation and the amount of entrained gas in the oil [10].

1.2.2.7 Oil Temperature

As the temperature of a liquid-gas mixture increases, gas effervescence (the escape of gas from a liquid) is observed. As dissolved air transforms into entrained air, the dissolved air content

decreases, which serves to increase the amount of entrained air. In a prior study it was observed that at 4000rpm, when the oil temperature increased from 100°C to 150°C, the entrained air bubble volume percentage doubled [7]. As the oil temperature increases, the associated decrease in viscosity (increased fluidity) permits imprisoned air to escape. Since entrained air can escape the mixture more easily at higher temperatures, this serves to decrease the entrained air content. As the engine speed increases, the oil temperature also increases. However, a decrease in oil aeration has not been observed during high speed and high temperature observation [7]. At a constant engine speed, as the oil temperature increases beyond 100°C, it has been observed that the oil aeration increases [11]. In a tank with an agitator, aeration was observed to decrease when the temperature was increased from 20°C to 100°C [12]. In another study, the gas bubble content was observed to increase with temperature from 80°C to 140°C at a constant engine speed, however the effect of temperature on aeration was smaller than that of increase in engine speed on aeration [10]. When the oil temperature increases, the oil viscosity decreases, and this serves to increase the oil flow through the lube system [6].

1.2.2.7.1 Bubble Size and Velocity

The difference between air density and oil density increases when the temperature rises. This causes the bubble size to increase because of the gas expansion. The bubbles rise velocity can be calculated from Stokes equation. Since the density differential and the bubble diameter both increase, the bubble's velocity increases [13]. Smaller bubbles rise very slowly and produce entrained air, while larger bubbles rise to the surface quickly and may transform into foam or escape the mixture.

According to [12], the size of a bubble at thermal equilibrium with the oil can be approximated by Boyle's Law,

$$PV = K .$$

Where, P is the pressure outside of the bubble, V is the volume of the bubble and K is a constant. The size of the bubble may vary due to the amount of air in the oil, but surface energy is always minimized, which results in a spherical bubble. LaPlace's Law describes the pressure inside the bubble.

$$P_b = P_{ext} + \frac{2\sigma}{R}.$$

Where, P_b is the pressure inside of the bubble, P_{ext} is the pressure surrounding the bubble, σ is the surface tension, and R is the radius of the bubble.

1.2.2.8 Oil Pressure

Dissolved air generally does not cause operational problems unless it leaves the oil solution. This occurs when the temperature rises or pressure decreases [4]. The air-oil mixture is no longer incompressible once the pressure falls below the saturation limit [5]. The solubility of air in oil is governed by Henry-Dalton's Law, which defines the equilibrium relation between the air pressure and the mole fraction of the dissolved air in the oil. Based on Henry-Dalton's Law, the volume of dissolved gas in equilibrium is directly proportional to pressure.

$$V_{gas} = B \cdot V_{liquid}\left(\frac{P + P_{atm}}{P_{atm}}\right).$$

Where, V_{gas} is the dissolved volume of gas under normal conditions (20°C, 101.3kPa), V_{liquid} is the volume of liquid under normal conditions, P is the pressure above normal atmospheric pressure P_{atm}, and B is the Bunsen Coefficient.

The dissolved air may be interpreted as a saturation limit for the solute (see Figure 1-6). The value of this limit increases with pressure. Thus, when the pressure increases, entrained air is absorbed into the oil solution. Likewise, when the pressure of a saturated air/oil mixture is reduced, a portion of the dissolved air leaves solution, forming entrained air bubbles. According to [9], the amount of soluble gas depends primarily on its chemical composition and the absolute pressure of the system. Engine oils at pressures below approximately 300bar comply with Henry-Dalton's law [9].

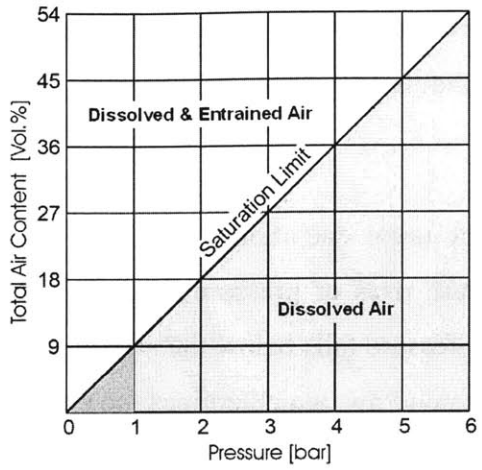

Figure 1-6. Air dissolving potential of engine oil [5]

The air solubility in engine oil is about 9% air volume percentage per bar of absolute oil pressure (Bunsen Coefficient-- The solubility may be represented by the Henry's Coefficient, the Bunsen Coefficient, or the Ostwald Coefficient. All of them are related. See [14]). Because of the weak temperature dependence, [6] reports that the Bunsen Coefficient is nearly constant for the range of temperatures encountered in a combustion engine. In general, the Bunsen Coefficient decreases as the temperature rises. As well, the Bunsen Coefficient depends on the oil specifications and additives; however 10% seems to be a common value for most modern oils [5].

1.2.2.9 Lube Path Oil Flow

According to [15], aeration affects the pump outlet pressure and thus the flowrate through the lube system. This occurs because aeration decreases the effective oil viscosity in the gallery. However, the decreased flowrate has less to do with the bubble size and more to do with the aeration level. In contrast, aeration increases the effective viscosity in the bearings (higher shear force to overcome the surface tension of the air bubbles). If the oil aeration increases above 25% at 3bar, the system pressure decreases. The engine oil pump volumetric efficiency is approximately 65% to 85% over the range of engine speeds and exit pressures corresponding to the lube system [15]. The volumetric efficiency is nearly constant above 3000rpm.

1.2.3 Effects of Oil Aeration

Oil is a coolant, lubricant, and working fluid in an internal combustion engine. Lash adjusters, chain tensioners and variable cam timing are hydraulically driven components that may be affected by aeration. When free air is in the high-pressure chamber of the lash adjuster, the stiffness is reduced and the adjuster may collapse under high load. This may cause the follower to miss the closing ramp on the cam and result in excessive valve closing velocities, noise and possibly failure [16].

Cavitation may occur in localized regions of low pressure. This primarily occurs in the pressure depression regions of the oil bores in the crankshaft, at the location of minimum distance from the rotating axis, due to a centrifugal effect. If dissolved air transforms to entrained air bubbles, this could inhibit the oil supply to the connecting rod bearings causing bearing failure due to lack of lubrication [6].

One of the main functions of engine oil is to cool engine components. If the oil contains entrained air, the thermal conductivity of the mixture is reduced, inhibiting the oil from properly cooling engine components.

Oil age has an indirect influence on oil aeration. Gas bubbles present at the oil pump inlet are compressed in the oil pump, forming explosive gas aerosols [5]. Ignition of the aerosols may occur, which results in an increased oil temperature. This serves to negatively influence the lubricant.

1.2.3.1 Foam Formation

"Foam formation has long been known to be an undesirable phenomenon. It reduces the strength of the lubricating layer, increases the tendency for oil to age, decreases the effective oil viscosity, density and thermal conductivity, and diminishes the oil pump performance, which results in reducing the rate of oil turnover" [17]. Foam formation may also cause the oil level to rise and come into contact with the crankshaft, which may impart a drag load on the crankshaft. Foam also produces a large liquid/air interface area, which facilitates the dissolution of air in the oil. Foam formation and stability are linked to the surface tension between the oil and the air. While

oil viscosity affects the oil film drainage process, its overall influence on foam formation and stability is not well established [18]. The stability of foams is a highly complicated phenomenon that depends on a number of parameters. The thin films separating gas bubbles may drain, the gas bubbles may rupture, or the gas bubbles may coalesce. Surface-active agents in the oil act as surfactants, which stabilize the foam against rupture [17]. The current state of understanding foam formation is not sufficiently advanced. As a result, unexpected and unexplainable cases of oil foaming are often met in practice [17]. A schematic of the air and oil interface is shown in Figure 1-7.

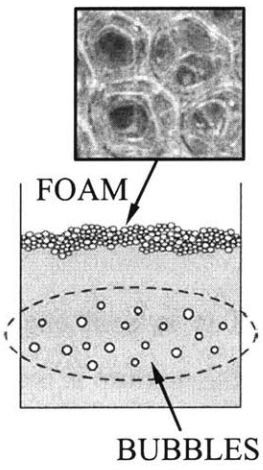

Figure 1-7. Foam and entrained air bubbles in a liquid

As the oil temperature rises, the viscosity decreases, promoting drainage of the lamellae. If the foam surface area increases (many small bubbles) or the change in surface tension with surface area increases, the film elasticity increases. As such, at low temperatures, the surface tension is greater than at higher temperatures. It is more difficult to collapse the foam layer at higher temperatures because the surface tension decreases relative to the fluid film. It is more difficult to form foams in higher viscosity fluids, however once formed, these foams are more difficult to break [3]. In an experiment by [7], the foam disappeared at 4000rpm, and more surface foam was observed at a low speed and medium temperature condition. Others cite falling oil viscosity at higher temperatures as the reason for decreased foam heights [17]. According to [5], the oscillating movement of the pistons causes a rapid gas exchange with the surface of the oil in the sump, and the consequence is a rapid rise in oil foam.

The foaming tendency is closely related to the change in oil surface tension in relation to the gas or vapor [17]. Some researchers believe that foaming increases with oil viscosity (Steinbach, 1959. See [17]), while others believe the opposite is true (Kohle, 1953. See [17]). Some researchers claim that the foaming tendency of oils changes in different ranges of viscosity. In lower ranges (4 - 128 mm^2/s) the foam formation decreases with increasing viscosity, while in higher ranges (128 - 325 mm^2/s) foam formation increases with increasing viscosity [17]. There is a distinction between the relationships governing foam formed by gases and those formed by vapors [17]. Foaming in vapors increases with temperature up to a certain point, after which it decreases, while gas foaming decreases with rising temperature, probably due to falling oil viscosity (Philippovich, 1960. See [17]).

1.2.3.1.1 Foam Tendency and Stability

Foaming tendency is a measurement of foam height after air has been bubbled through a sample of oil maintained at a specific temperature for a specific period of time [ASTM D-892]. It is more difficult to form foams in higher viscosity fluids. As such, as the temperature rises, the oil viscosity decreases allowing foam to form. Foam height has been observed to decrease, at a constant oil temperature, as the engine speed increases [7]. However, this may be a result of the droplet destruction mechanism presented in [19]. Different trends were observed between [17] and [3], however [3] spoke of fluids in general and [17] discussed oils. It should be noted that both of these studies ([3] and [17]) were not performed in the oil sump of an operating engine.

In the second phase of the ASTM D-892 test, the foam is allowed to dissipate for ten minutes and the volume of foam is measured and reported as the foam stability. In a test environment, for many different oils, the foam stability has been cited to decrease as the temperature increases [3]. One logical explanation is the decreased oil viscosity in the elastic film that may tend to drain more quickly as the oil viscosity decreases. The foam stability has also been cited to increase as the surface tension between the gas-air interface decreases. Since surface tension decreases with temperature, this should promote foam stability in an engine. Though this has not been verified experimentally.

The foam tendency and foam stability can change with time in service. Newer oils will have a lower tendency to foam and a lower foam stability values, and contaminated oils will have an increased tendency to foam [3]. An equilibrium foam height can be observed if the rate of gas release from the foam is equal to the rate of gas flow into the foam [20].

1.2.3.2 Connecting Rod and Main Bearings

An analytical development by [21] showed that oil aeration increases the load capacity of plain journal bearings with a negligible reduction in oil film density. The oil viscosity is expected to diminish with increasing aeration rate due to the negligible internal viscosity of the entrained air bubbles. However, a bearing surface experiences additional drag because work is required, against surface tension, to shear the spherical bubbles into ellipsoids. Therefore, oil viscosity in the bearings has been observed to increase with oil aeration. The predicted viscosity increase was also observed by the experimental findings of [22]. A summary of relevant oil aeration research relating to density and viscosity models was prepared by [23]. The oil film pressure increased as the aeration increased [23]. This can be attributed to the viscosity rise resulting from the increasing surface tension caused by the increase in the number of bubbles.

Oil aeration takes place during engine start-up, under high-speed operation, or under sharp vehicle maneuvers. The change in minimum oil film thickness in the bearings was very small up to a 30% aeration rate, but at greater aeration rates, the thickness varied [24]. In the high-pressure regions of the bearing, the diameter of air bubbles was reduced. This results in minimal deterioration of the load carrying capacity. The crankshaft temperature increased as a result of the viscous shear of the lubricating oil between the shaft and the bearings, which is closely related to the oil film thickness.

1.2.3.3 Hydraulic Lash Adjusters

Hydraulic lash adjusters (HLA) are placed between the cam and the valve, ensuring contact between the cam and the valve. As the near incompressible oil is aerated, the compressibility of the air/oil mixture affects the operation of the hydraulic lash adjusters [25]. A method of calculating the air fraction in the high-pressure chamber of the HLA was developed by [26]. Thus, the HLA serves as another engine component whose operation is dependent upon the level of engine oil aeration.

Chapter 2: Engine Set-up and Test Apparatus

A production Ford 3.0L V6 DOHC engine was used in this study, and aol aeration was observed without firing the engine. As such, a 75hp motor with variable speed control motored the engine. The maximum motor speed was 3600rpm, thus it was necessary to couple the engine to the motor via a *Ramsey Silent Chain* assembly (RPV-308, 9.525mm pitch, 50.8mm face width, 2.29 gear ratio) as shown in Figure 2-1. The chain enabled the engine to be motored to a maximum speed of 8000rpm.

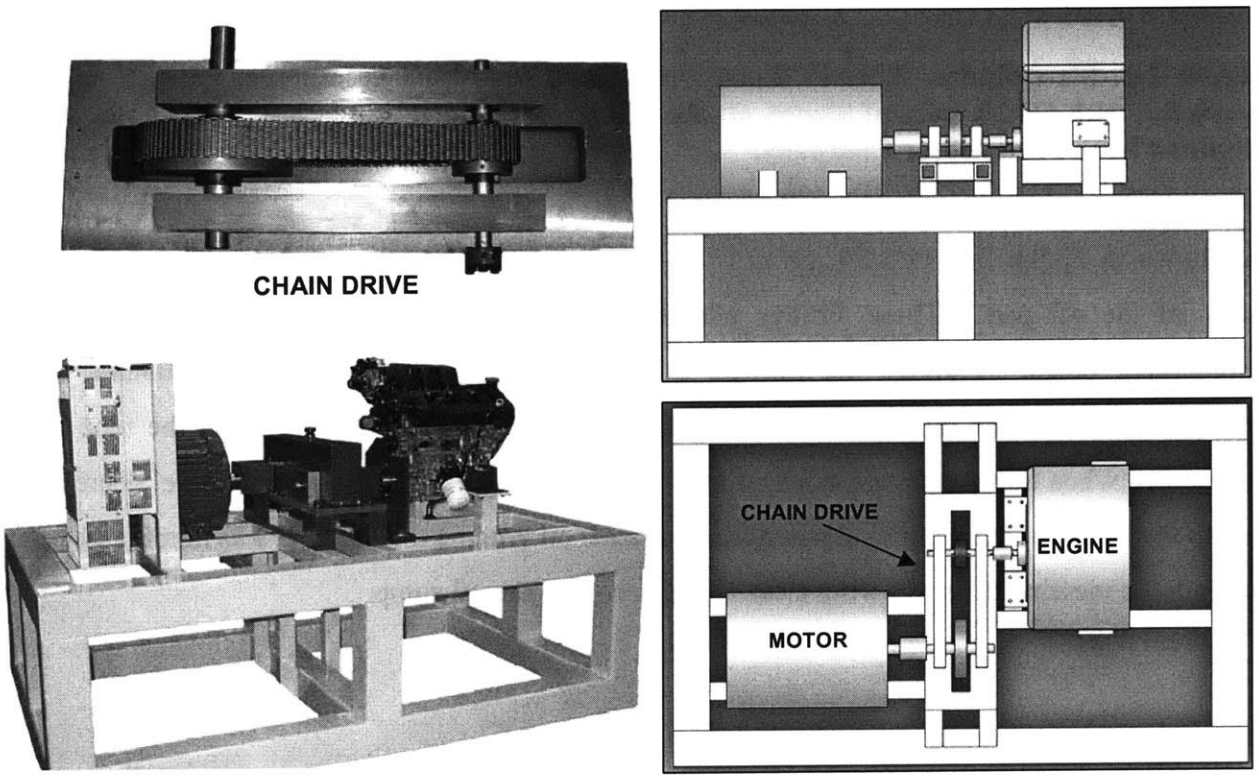

Figure 2-1. Test structure, chain drive, and test apparatus schematic

The oil pan was modified to allow passage of a borescope into the sump. Data obtained from a firing engine were used to design the necessary oil pan modifications. The oil sump temperature and pressure for a firing Duratec engine are shown in Figure 2-2.

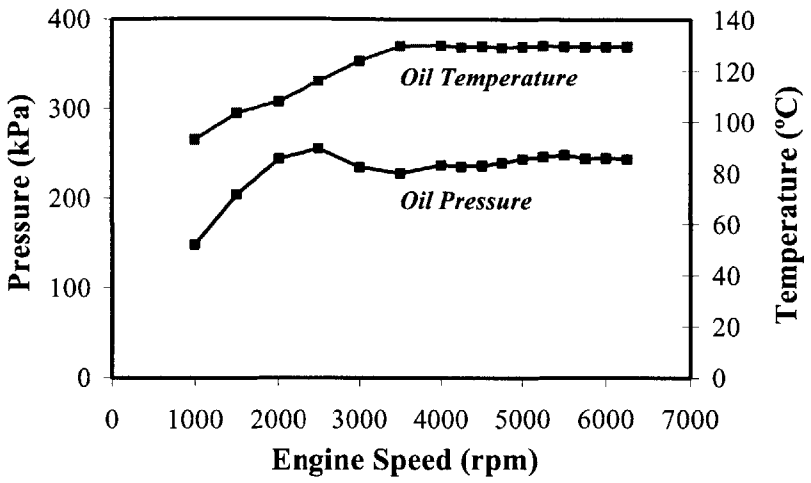

Figure 2-2. Six-cylinder, 3.0L-4V Ford *Duratec* oil operating conditions. Firing engine operation with 5W20, bore of 89mm, stroke of 79.5mm, and compression ratio of 10. Data obtained from Ford Motor Company.

As shown in Figure 2-3, two *Swagelok Ultra-Torr* vacuum fittings were installed on opposing sides of the oil pan. These fittings allowed repeated disconnects and a broad operating temperature range. Through the fittings, a 12.7mm OD (9.525mm ID) polycarbonate tube spanned the oil pan at mid-span. The height of the tube passage was such that the tube was submerged when the engine was not running. When the engine operated, the oil level decreased due to the filling of the engine oil passages. For a 4L oil volume the oil level was nominally 1cm beneath the viewing tube, allowing clear visual access to the oil sump.

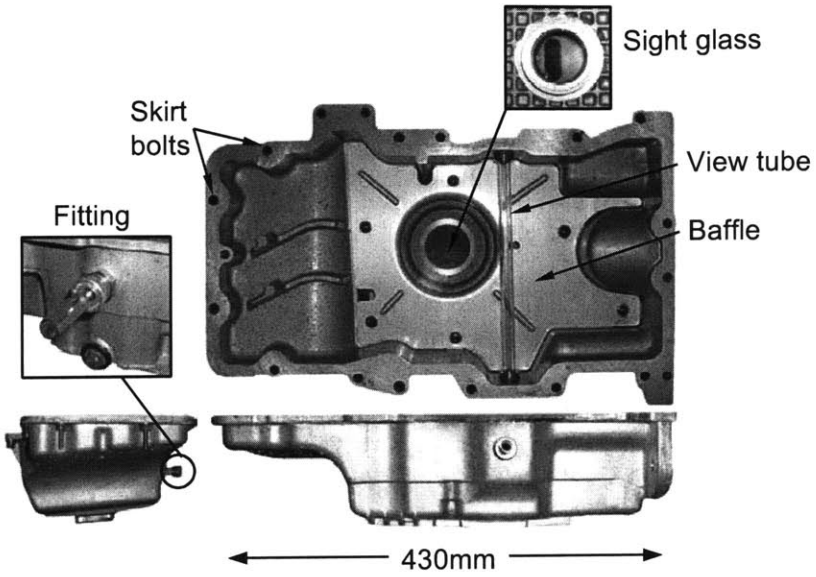

Figure 2-3. Oil pan and transparent viewing tube

Visual observation was done via an *Olympus Series V* borescope with a 90° viewing angle and a line of sight perpendicular to the probe axis. The probe was used in conjunction with an *Olympus ILX-6300* Xenon High Intensity Light source. A *Vision Research Phantom 4.2* high-speed camera, capable of capturing videos at frame rates of up to 90,000fps (32 x 32 resolution), was used. At 512 x 512 resolution, this camera is capable of capturing images at 2,100fps, which translates into approximately 1.2 frames/CAD at 1000rpm. The camera and borescope are shown in Figure 2-4.

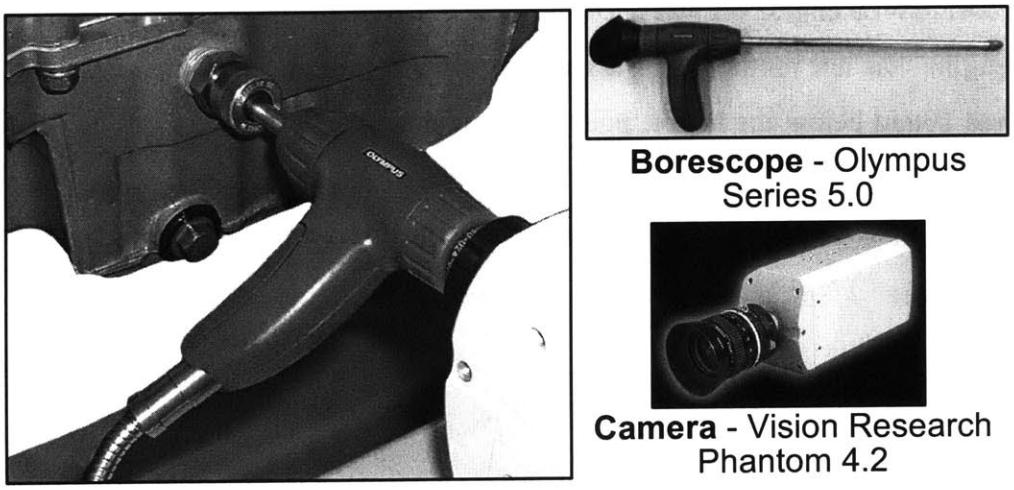

Figure 2-4. Set-up of borescope and camera

The engine was instrumented with thermocouples and pressure gauges to monitor transient and steady conditions. The gas in the cylinder, exhaust gas, cooling water outlet, and oil gallery temperatures were monitored, as were the inlet water and oil gallery pressures. Filtered cooling water at 25°C (420kPa) was circulated through the engine block and head. The cooling water was not recycled. A schematic of the four thermocouple temperature measurements (T) and two pressure gauge measurements (P) is shown in Figure 2-5. The oil gallery temperature was continuously monitored during video acquisition.

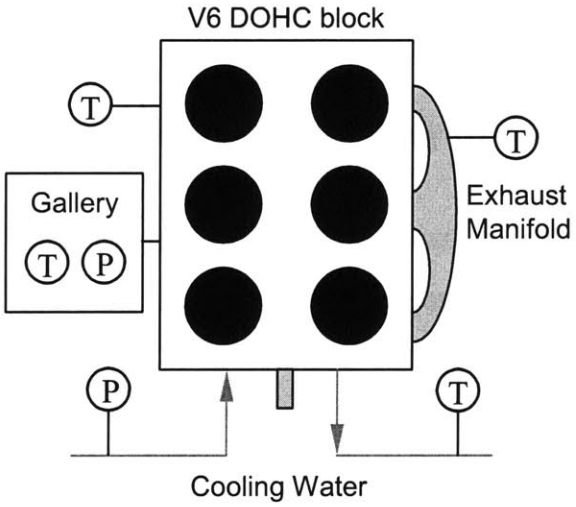

Figure 2-5. Schematic of engine instrumentation

Motorcraft SAE 5W20 engine oil was used for these experiments (See Table 2-1 for properties). When the engine was not running, an oil volume between four and five liters resulted in an oil level that was 10mm below the lowest point of the counterweight trajectory. Four to five liters of oil were used in these visualization experiments. During engine operation with 4L, approximately 2.2L of oil remained in the sump, while the rest occupied the engine oil passages.

Table 2-1. Engine oil specifications (courtesy of www.motorcraft.com)

SAE Grade	5W-20
API Service	SJ / EC
Gravity	35 °API
Density, @ 15.5°C	851 kg/m^3
Flash Point, COC	185 °C
Kinematic Viscosity at 40°C	4.9×10^{-5} m^2/s
Kinematic Viscosity at 100°C	8.8×10^{-6} m^2/s
Viscosity Index	161
HT/HS Viscosity @ 150°C	2.65 cP
Pour Point	-45 °C
Sulfated Ash	0.94 Wt. %
Total Base Number	7.5 TBN
ASTM Color	4

Additional instrumentation was added to the test apparatus. To ensure a smooth start-up and shut-down, spark plug valves were added to the cylinders. In addition, when the valves were open at speeds below 1500rpm, the torque generated by the motor remained steady. If the spark plug valves were closed below 1500rpm, undue cyclic loading on the couplings was observed. The throttle was removed from the engine to ensure that wide-open throttle conditions were examined in all cases. At engine speeds beyond 6000rpm, the noise generated from the exhaust was partially muffled by the exhaust manifold. For the visual observation experiments, the gallery pressure and temperature were monitored. The test engine is shown in Figure 2-6.

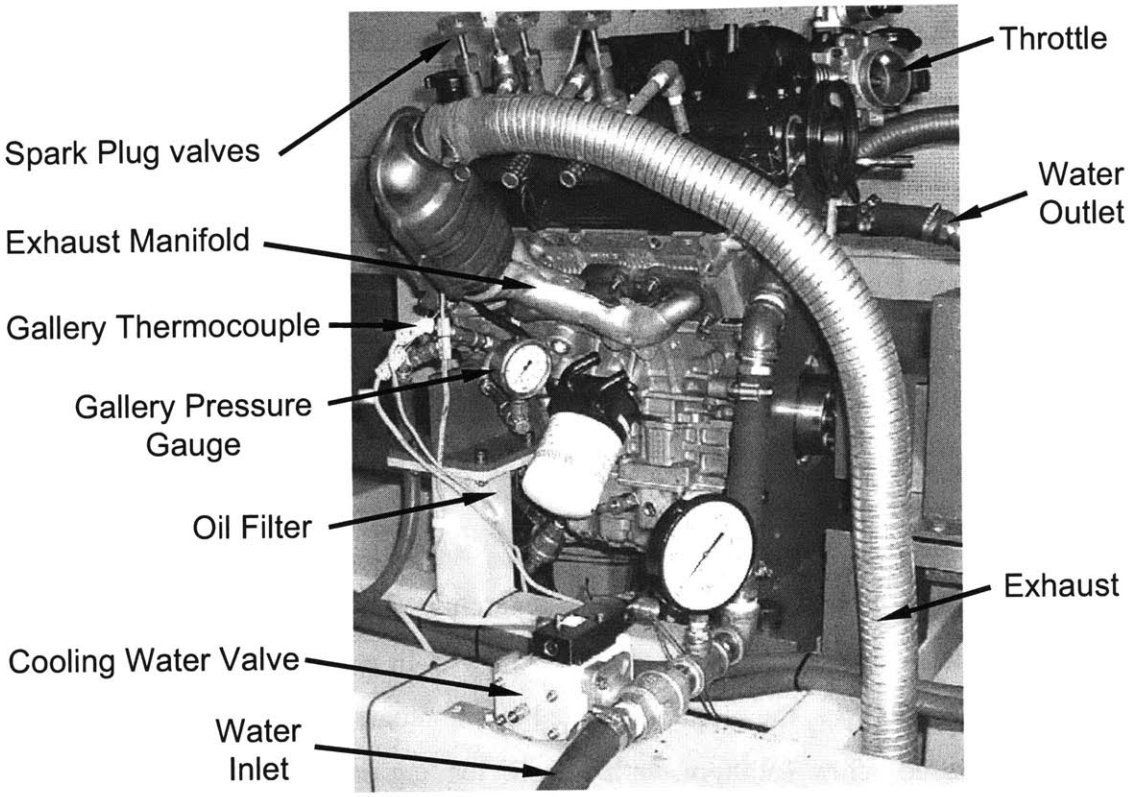

Figure 2-6. 2003 3.0L DOHC motored Ford *Duratec* aeration test engine

Pneumatically actuated ball valves were used to control the cooling water supply and the oil sampling locations in the sump. This valve is shown in Figure 2-7.

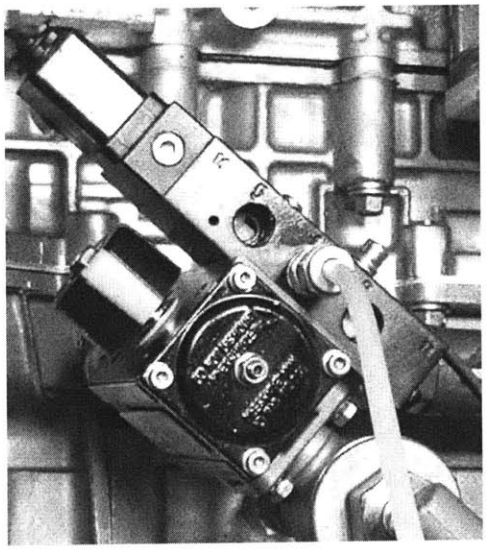

Figure 2-7. Pneumatically actuated ball valve

From beneath the engine (looking upward through the windage tray), the oil pump transports the oil from the sump through the pick-up (see Figure 2-8). When the pressure in the oil lube system exceeds a specified value, the pump relief valve opens, returning oil to the sump. The crankshaft drives both the left and right timing chains. Three oil returns (one returning oil from the left head and two returning oil from the right head) are shown in Figure 2-8. The windage tray is also shown, separating the crankshaft from the oil in the sump.

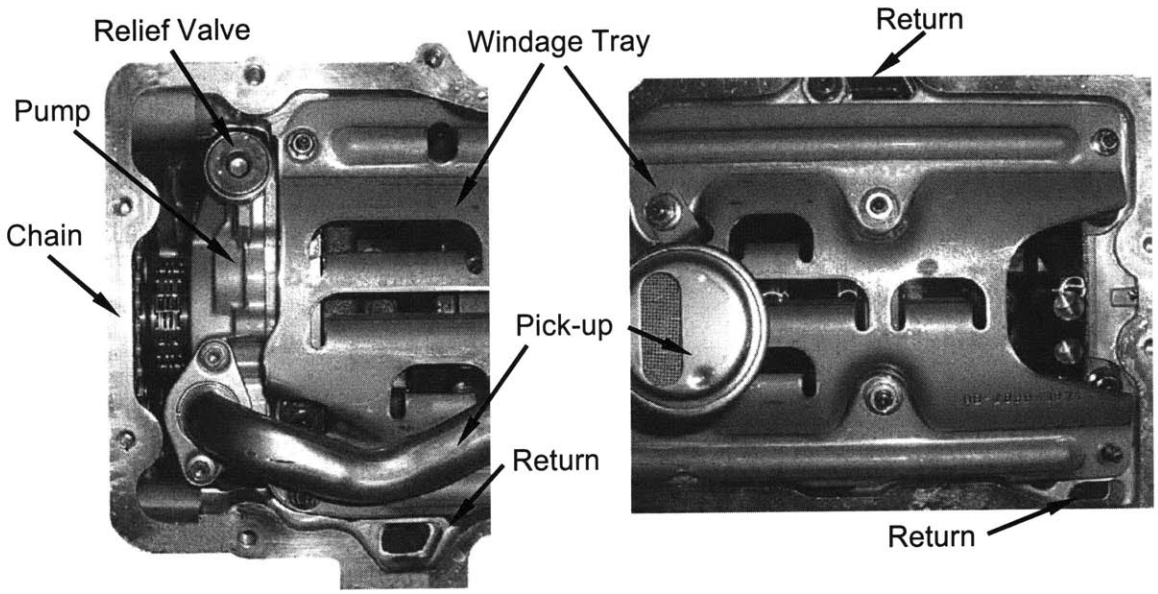

Figure 2-8. Looking upward from the oil sump through the windage tray

(This page is intentionally blank)

Chapter 3: High Speed Video Observation of Oil Aeration

Engine oil serves multiple functions within an engine, from lubricating and cooling to acting as the working fluid in hydraulic systems. The presence of air in the oil (oil aeration) can be detrimental to many of these functions. This chapter describes the visual observations of air/oil interaction in the crankcase. The effort is focused on the processes in the sump, which are believed to be the main source of introducing air into the oil.

The oil aeration process in the crankcase was visualized with a high-speed video camera and a borescope at engine speeds up to 4000rpm and oil temperatures below 100°C. The video images revealed a high-speed oil droplet stream being flung from the crankshaft counterweight. These droplets passed through the oil drainage gap in the windage tray and struck the free surface of the oil in the sump. There was a speed threshold beyond which foam was observed to form on the oil surface. When the engine speed was reduced to below that threshold, the foam disappeared. When the windage tray was removed, there was no foam formation. The results suggested that foam formation was the net result of the balance between the air bubble formation and destruction processes. These two processes were speed dependent.

3.1 Visualization Geometry

Before visual observations are presented it is important that the various viewing angles are described in detail. Since oil droplets are the primary visual observation in the oil sump, an explanation of their origin is of importance. Oil from the main gallery is received by the main bearings, and through oil bores in the crankshaft fed to the connecting rod bearings. A typical crankshaft is shown in Figure 3-1.

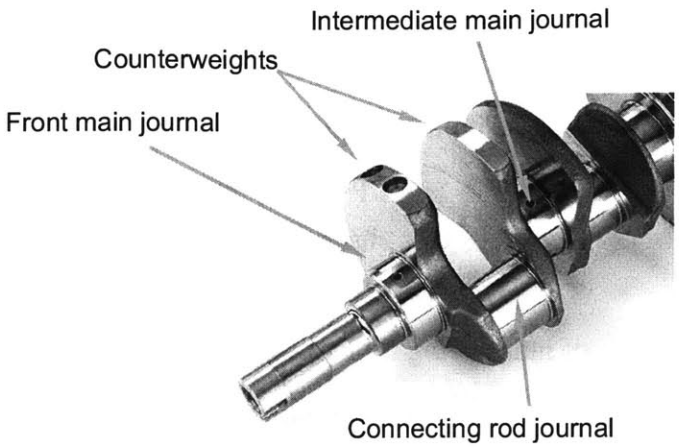

Figure 3-1. Engine crankshaft (courtesy of www.autospeed.com)

A common viewpoint for visual observation is looking upward from the viewing tube through a passage in the windage tray. From beneath the engine looking upward, the windage tray can be seen as a divider between the crankshaft and the oil pan. A crankshaft counterweight can be seen through an individual passage in the windage tray (see Figure 3-2).

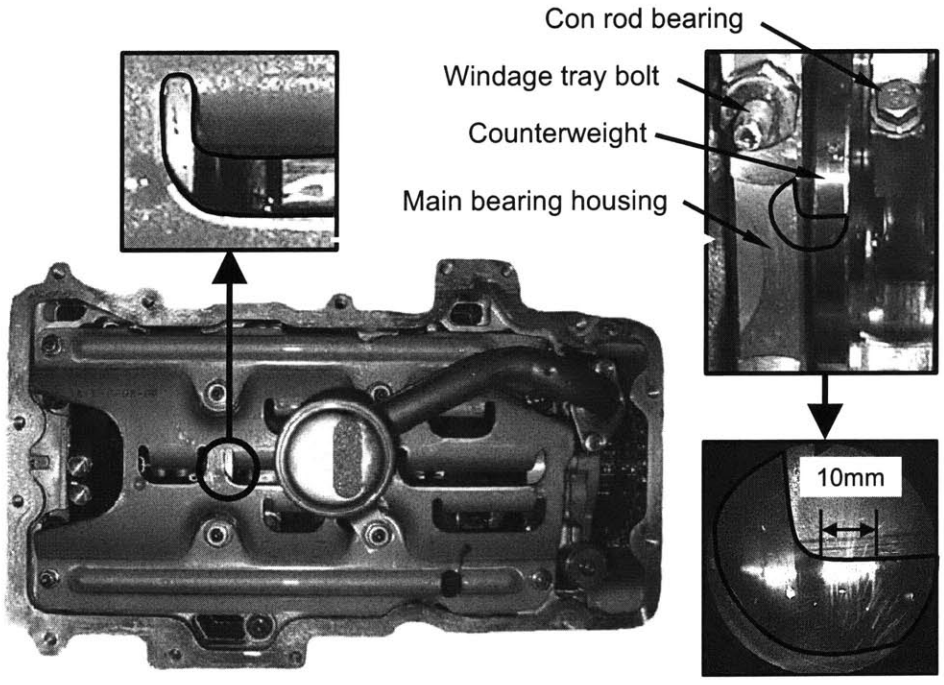

Figure 3-2. A crankshaft counterweight as seen through the windage tray

A second viewpoint is looking to the rear of the oil pan from the viewing tube. From this vantage point, the droplet dynamics can be observed as well as the interaction between the droplets and the free surface of the oil. An example image captured from a high-speed video is shown in Figure 3-3.

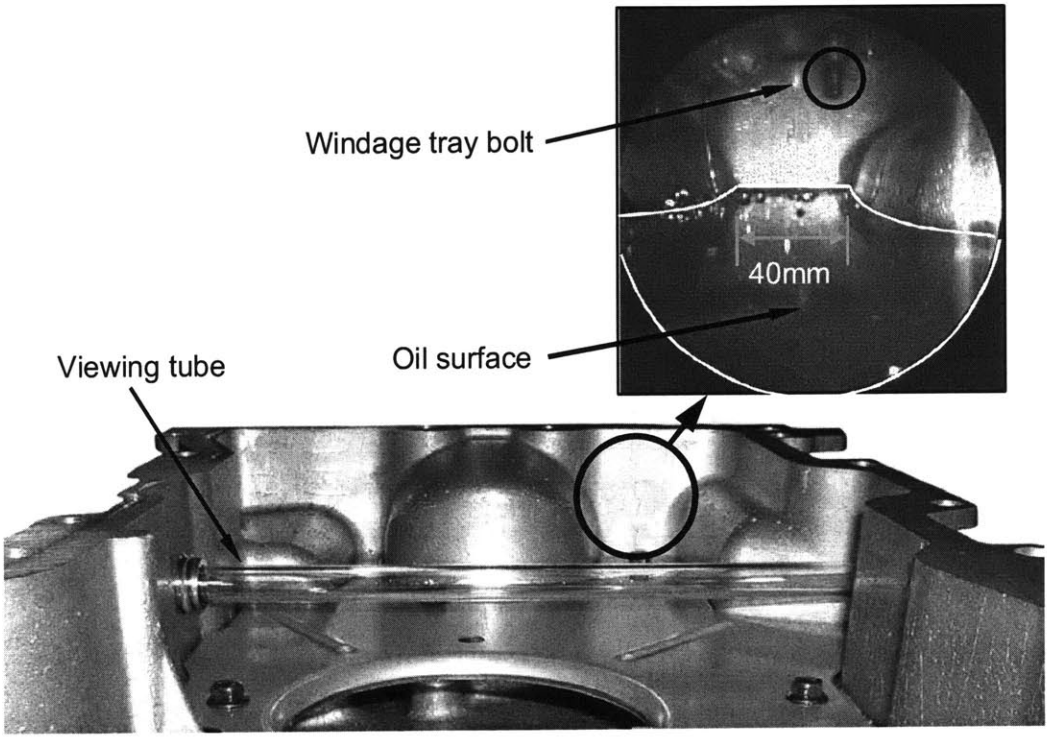

Figure 3-3. Rearward oil sump view from the viewing tube

3.1.1 Oil Pan Geometry

The geometry of visualization is shown in Figure 3-4. In the video capture experiments, the borescope was positioned longitudinally in the viewing tube at three locations. Referring to Figure 3-4, for positions A and B, the view was upwards through the oil drainage gaps in the windage tray. For position C, the view was sideways towards the rear of the oil pan.

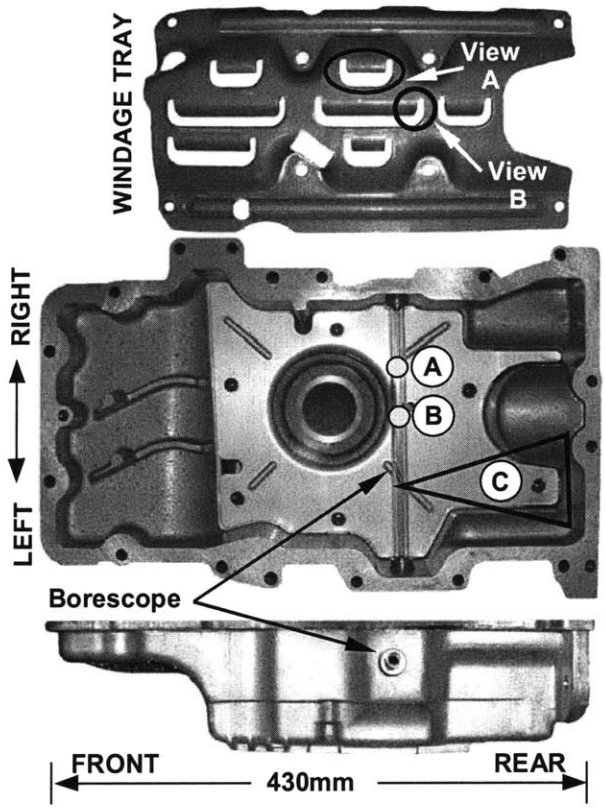

Figure 3-4. Oil pan visualization geometry

During visualization, the engine speed was limited to 3000rpm, which was substantially lower than the maximum engine motoring speed. This limitation was a result of two observations. At higher engine speeds, many droplets landed on the tube and obscured the view. Secondly, if a significant amount of foam was formed and the tube was submerged in the foam, the view was also obstructed. During either of these two conditions, observations of the crankcase events were difficult.

3.2 Qualitative Examination of Oil Aeration

To examine the effect of the windage tray on oil aeration, the tray was removed in some of the experiments. Unless otherwise noted, all experiments were performed with the windage tray present.

In the following discussion, the crankcase events are described in terms of static images extracted from high-speed videos. The videos were acquired after the engine reached a steady-state motoring condition (stable speed and oil gallery temperature). It should be noted that these static images do not fully convey the dynamic nature of the events as captured by the high-speed videos. Much of the dynamics are described in the narratives.

3.2.1 Windage Tray

The windage tray is sometimes referred to as a baffle or a scraper; it performs both of these functions. The windage tray prevents oil in the sump from splashing and coming into contact with the crankshaft. Passages or gaps in the windage tray allow for oil drainage. Grooves exist atop the tray to direct oil to these gaps. Since there is less than 5mm clearance between the counterweights and the windage tray, the tray acts as a scraper, receiving oil that is spun off the counterweights (see Figure 3-5).

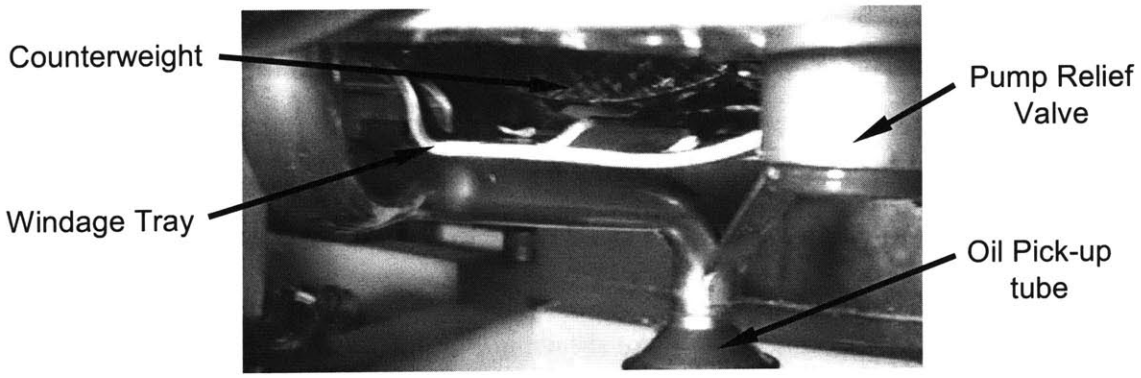

Figure 3-5. Counterweight, windage tray, and oil pick-up tube

Figure 3-6 shows the view from position A upwards through the oil drainage gap in the windage tray (see Figure 3-4 for geometry). The engine was operating at 1370rpm. The crankshaft counterweight can be seen through the gap. Small droplets (shown as streaks in Figure 3-6) were flung through the gap in the windage tray at approximately the tangential velocity at the maximum radius of the counterweight; the value at 1370rpm was 12m/s. These high velocity droplets interacted with the oil free surface substantially.

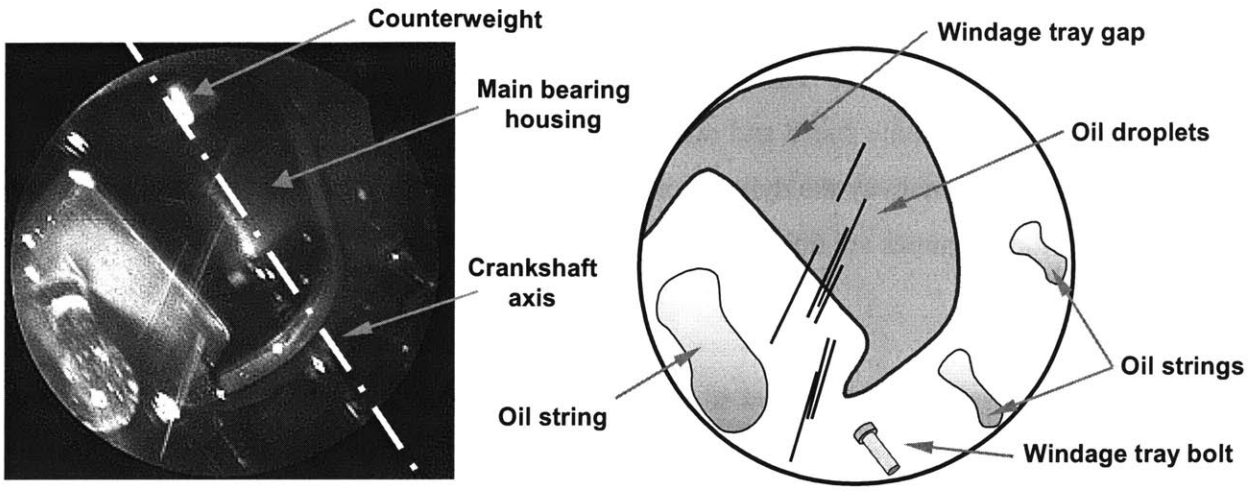

Figure 3-6. Oil droplets flung from the crankshaft counterweights; oil strings dripping off the windage tray. Engine speed of 1370rpm, 30°C gallery temperature (recorded at 500fps, 256x256 pixel resolution; Viewed from position A looking upwards).

Atop the tray, the oil pooled and flowed to nearby passages. This oil then drained to the underside of the tray. The oil mass collected at the edge of the gap or the underside of the windage tray until it was large enough to string itself out and drain into the sump. Many of these "strings" with diameters on the order of millimeters can be seen in Figure 3-6. The velocity of the resulting millimeter size strings landing on the oil pool in the sump was less than 1m/s. These strings did not sufficiently agitate the free surface to produce significant air entrainment.

The oil drops flying off the counterweight are shown in Figure 3-7 at different engine speeds. At 1500rpm, before the appearance of the counterweight through the windage tray gap, relatively few droplet streaks were observed (top left image in Figure 3-7). Substantially more droplet streaks appeared with the arrival of the counterweight (see the middle left image, which was taken at about the mid point of the counterweight passage). The droplets were traveling in the crankshaft tangential direction. Soon after the passage of the counterweight (bottom left image in Figure 3-7), a substantial number of droplets were still observed. This observation suggests that the droplets flung off the counterweight were traveling slightly slower than the tangential velocity of the counterweight; hence there was a "trail" of droplets.

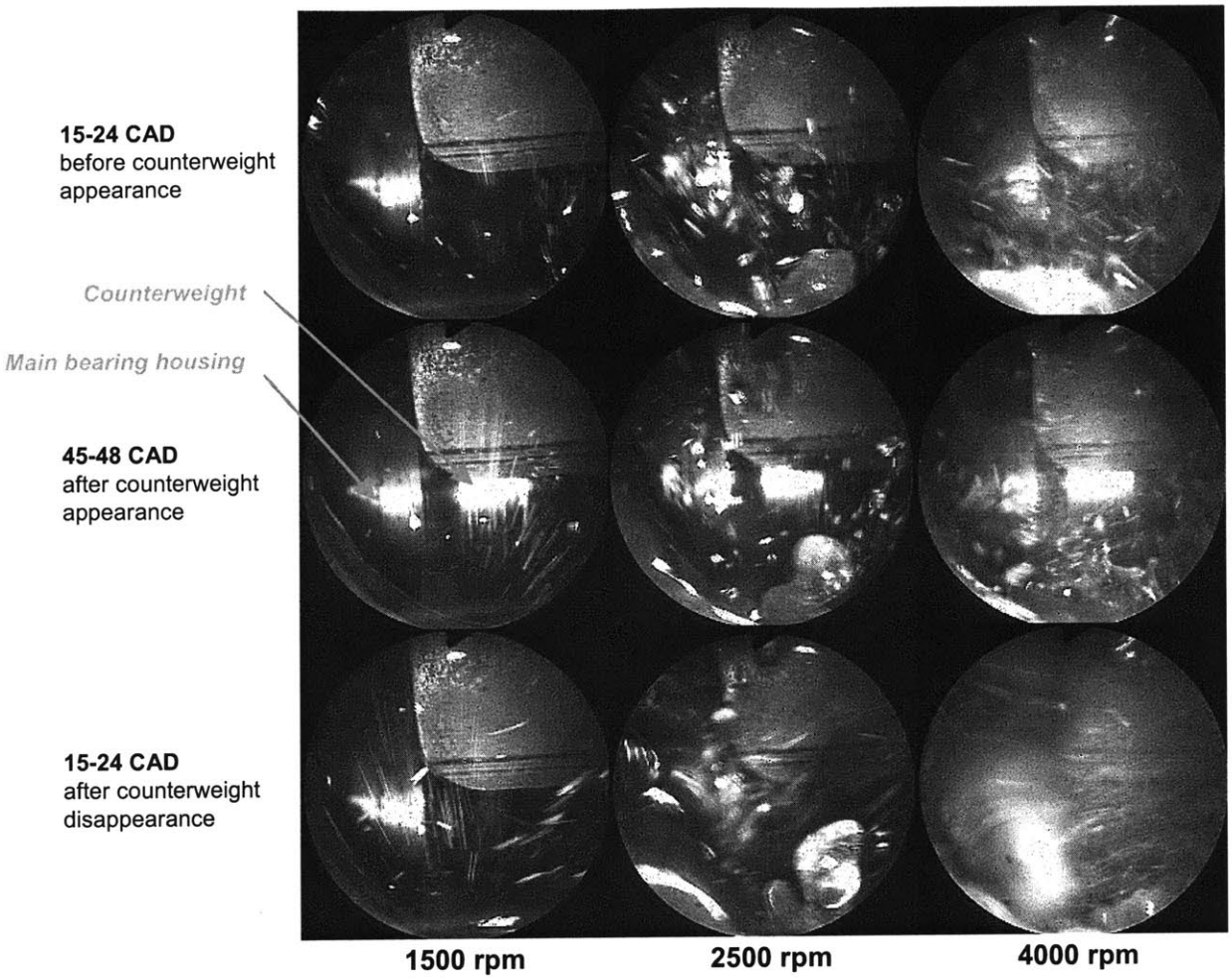

Figure 3-7. Counterweight as seen through the windage tray gap (video captured at 2000fps, 256x256 pixel resolution and viewed from position B looking upwards).

At 2500rpm, the situation was qualitatively the same, except that there were more droplets and the droplets were traveling faster; see center column images of Figure 3-7. Images were obtained at an engine speed of 4000rpm (third column of Figure 3-7). At this engine speed, there were a large number of oil drops landing on the view tube. The view was frequently obscured due to oil accumulation from these droplets and the subsequent clearing by oil drainage; see bottom image of the right column in Figure 3-7. Observation from the high-speed video showed that there was a sloshing of this accumulated oil, driven periodically by the oil drops flung from the crankshaft (see Figure 3-8). The frequency of the sloshing was the same as the rotational speed of the crankshaft.

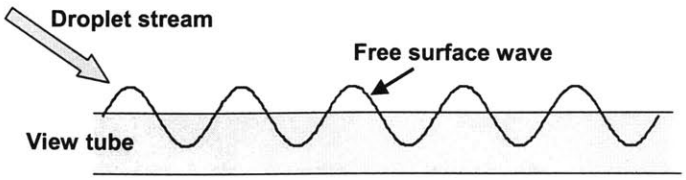

Figure 3-8. Surface waves excited by the droplet stream flung off from the counterweight

The overall level of droplet number density in the sump was monitored by looking at the rear region of the oil pan, shown as position C in Figure 3-4. This view is shown in Figure 3-9(a), which was taken at 2000rpm. Droplets were observed to bounce on the oil free surface before merging with the oil.

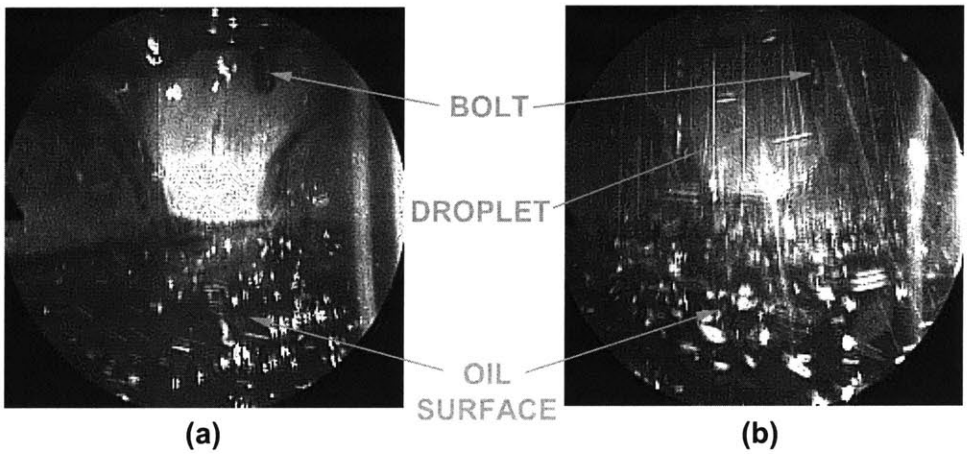

Figure 3-9. Oil droplets in sump at 2000rpm; (a) With a windage tray, and (b) Without a windage tray. View from position C.

When the windage tray was removed, the droplet number density increased substantially as shown in Figure 3-9(b). The image confirmed that the windage tray prevents the majority of the fast moving droplets from entering the sump.

Oil re-enters the sump as droplets passing through the holes in the windage tray or as oil draining through the windage tray. As the crankshaft rotated, oil was flung in all directions. However, the windage tray shielded many of the droplets from entering the sump. A panoramic image was created showing the rearward view of the oil draining back into the sump (see Figure 3-10). On the left side of the image, a larger portion of oil entered the sump as compared to the right side of

the image. Looking in the rearward direction, the crankshaft rotates clockwise, thus indicating that the crankshaft dragged oil across the windage tray, which resulted in a disproportionate distribution of oil draining back into the sump.

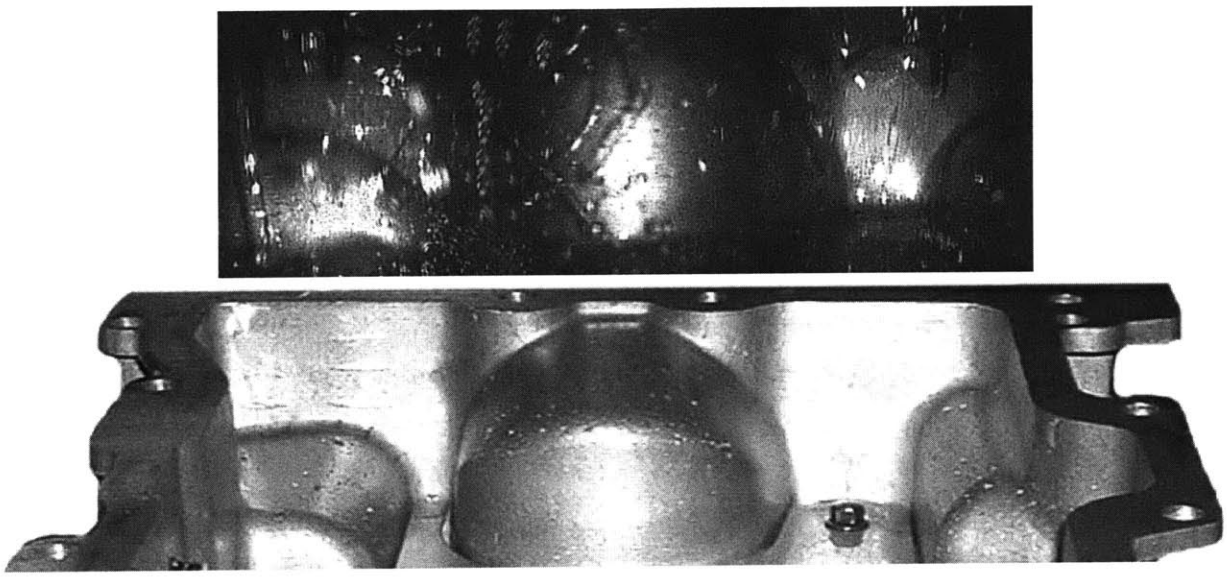

Figure 3-10. Oil from the crankshaft draining back into the oil sump (engine speed of 2000rpm and an engine oil temperature of 50°C)

It was evident that not only the oil droplet dynamics depend on the windage tray, but also the oil flow back into the sump.

3.2.2 Modifying the Windage Tray

Some of the oil leaving the con rod and main bearings re-enters the oil sump as droplets flung from the crankshaft. As a means of isolating the aeration and foaming mechanisms, the windage tray was modified to reduce the oil passage area, which reduced the number of droplets that pass freely through the passages in the windage tray. The original and modified windage trays are shown in Figure 3-11.

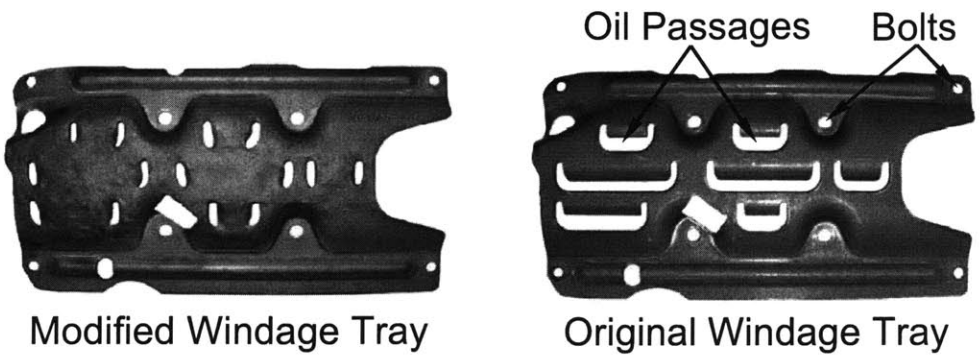

Figure 3-11. Modified and original windage tray

Qualitative visualization experiments were performed and it was found that the modified windage tray did not serve to reduce the droplet number density. This suggests that droplets were still able to strike the free surface of the oil in the sump by passing through the holes in the modified windage tray.

3.2.3 Oil Droplet Behavior

The droplets departing the crankshaft passed through the gaps in the windage tray and struck the free surface of the oil. In a similar fashion as the original windage tray, a group of droplets detached the counterweight and entered the sump through a passage in the modified windage tray (see Figure 3-12).

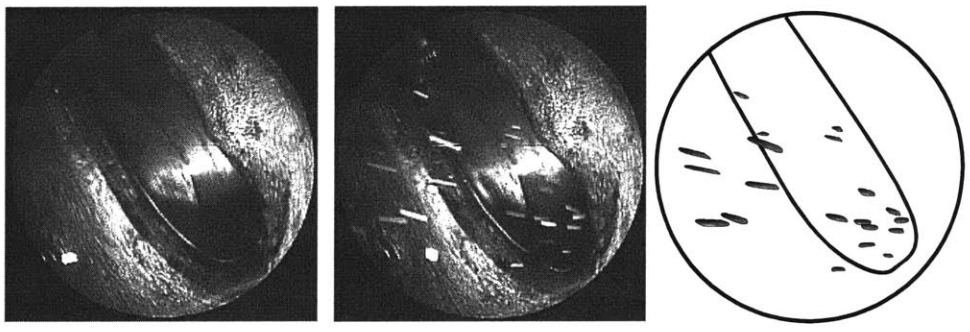

Figure 3-12. Oil droplets flung from the counterweight at an engine speed of 800rpm and an oil gallery temperature of 40°C (viewed through a hole in the modified windage tray).

After an individual droplet passed through either the modified or original windage tray, the droplet collided with the free surface of the oil in the sump (see Figure 3-13).

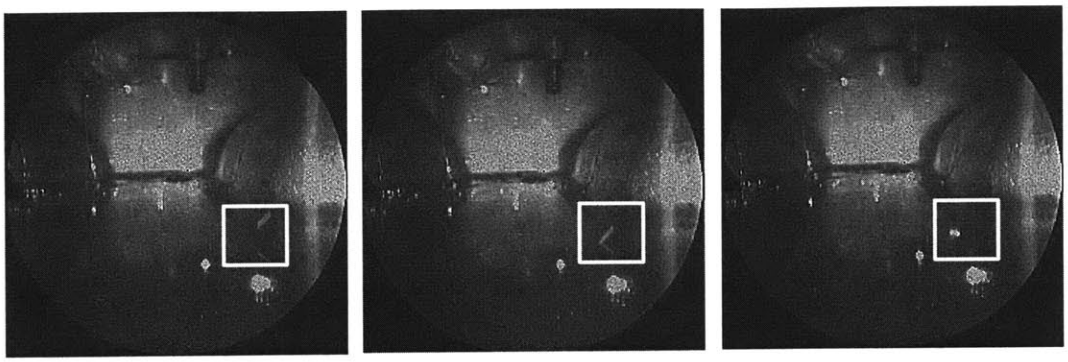

Figure 3-13. Consecutive images of an oil droplet colliding with surface of the oil (800rpm, oil gallery temperature 30°C, 256x256, 500fps)

It is thought that the interaction between the droplet and the oil surface may be a mechanism for aerating the oil. An image of a droplet striking the oil surface was obtained beneath the surface of the oil. As the droplet impacted the surface, the oil formed a crater and stem as shown in Figure 3-14. After forming, the crater disappeared and none of the air occupying the inside of the stem was trapped in the bulk of the oil.

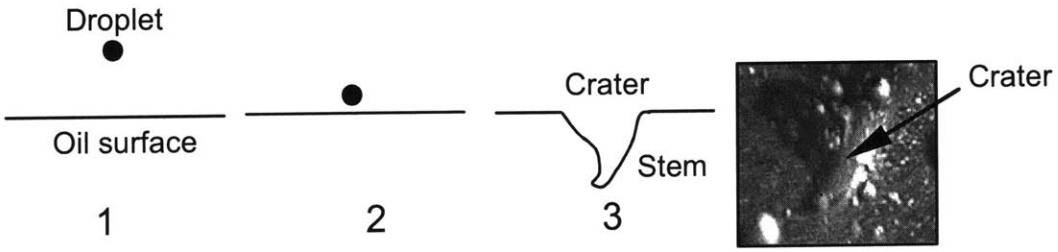

Figure 3-14. Schematic of a droplet striking the oil surface

Visual observations reveal minimal dynamic interaction between the droplet and the oil surface, however visualization was performed at engine speeds below 4000rpm.

3.2.4 Foam Formation

In a number of experiments over a range of engine speeds, foam formation was first observed at 2000rpm and the amount of foam in the oil sump increased with time until an equilibrium level was reached. This process is shown in Figure 3-15. At speeds below 1500rpm, no foam

formation was observed. At 2000rpm, foam started to form in the oil sump (see image (iii)). As time progressed, the amount of foam increased; see image (iv), which was taken approximately 300s after the engine speed was increased to 2000rpm. At the time of image (v), which was taken approximately 400s after the speed change, the foam level had increased to the height of the viewing tube and obstructed the view.

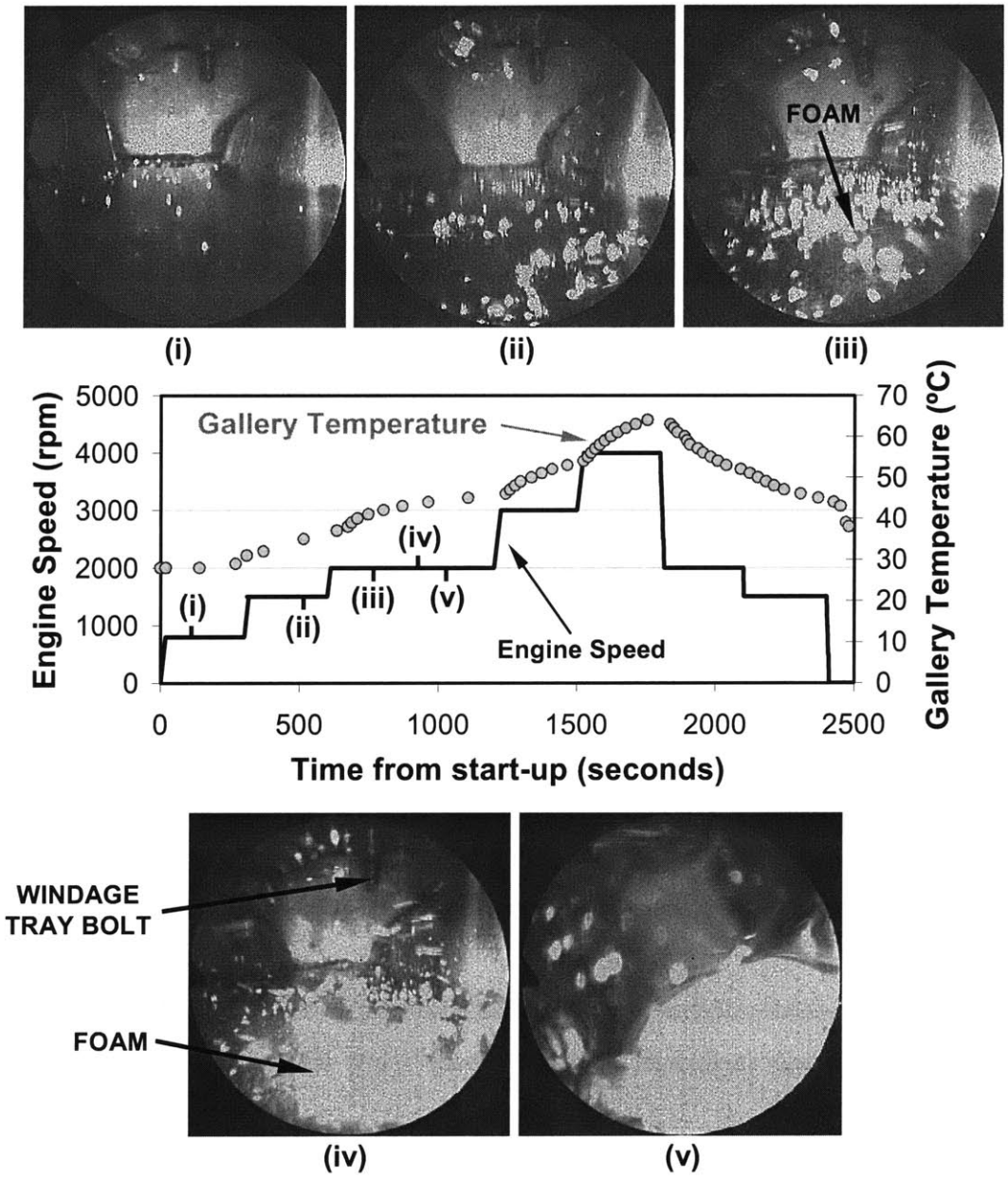

Figure 3-15. Foam formation at 2000rpm (original windage tray and 4.5L of oil)

When the engine speed was subsequently increased to 4000rpm and then decreased to 1500rpm, the foam growth persisted and the foam level continued to engulf the viewing tube and obstruct visual access. However, approximately 100s after the speed was reduced to 1500rpm, the viewing tube was no longer covered with foam and a clear view similar to the Figure 3-15(ii) was observed. The same experiment was performed without the windage tray. There was evidence of foam formation, when experiments were performed without the windage tray, at the low speed (below 4000rpm) and low oil temperature (below 70°C) operating conditions.

The presence of foam on the oil surface may be discussed in terms of the foam formation and destruction processes. The foam was formed from the accumulation of air bubbles rising to the surface. It was destroyed by the foam film drainage and by the piercing of the foam bubble by the droplets flung from the crankshaft. An example of the latter process is shown in Figure 3-16.

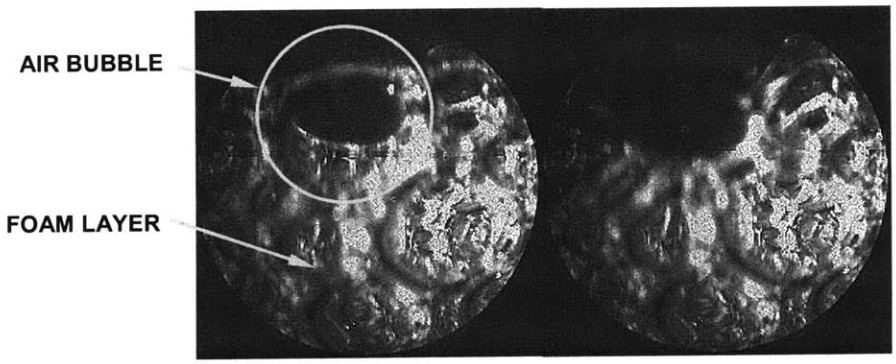

Figure 3-16. A bubble in the foam was destroyed by an incoming oil droplet at an engine speed of 2000rpm and an oil temperature of 54°C.

The processes that create and destroy the air bubbles in the sump are listed in Table 3-1. The effects of the engine speed on these processes are also listed. Thus the presence of foam depended on the competition between the formation and the destruction processes, the rates of which are dependent on engine speed in a non-linear manner. The net result is a speed threshold for foam formation.

Table 3-1. Processes that create and destroy air bubbles in the oil sump

AIR BUBBLE CREATION	EFFECT OF A SPEED INCREASE
(a) Air entrainment as result of surface agitation by the oil droplets flung from the crankshaft	Increase in aeration; although less effective after foam formation.
(b) Release of dissolved air from the oil in the sump	Probably an increase in aeration due to the increase in oil temperature, although this trend could not be inferred.
AIR BUBBLE DESTRUCTION	**EFFECT OF A SPEED INCREASE**
(i) Gravitational drainage of the foam film; drainage increases with foam height	Neutral
(ii) Puncturing of bubbles by the flying oil droplets	Increase in aeration because of the increase in droplet number density.
(iiii) Ingestion of air bubbles by the sump pump	Increase in aeration because of the decrease in oil sump resident time.

Foam formation was observed at a constant engine speed. At 2000rpm, the oil temperature increased to above 100°C. From experimental data for a firing engine, the oil temperature at 2000rpm is approximately 110°C. Three images captured from the high-speed video are shown in Figure 3-17.

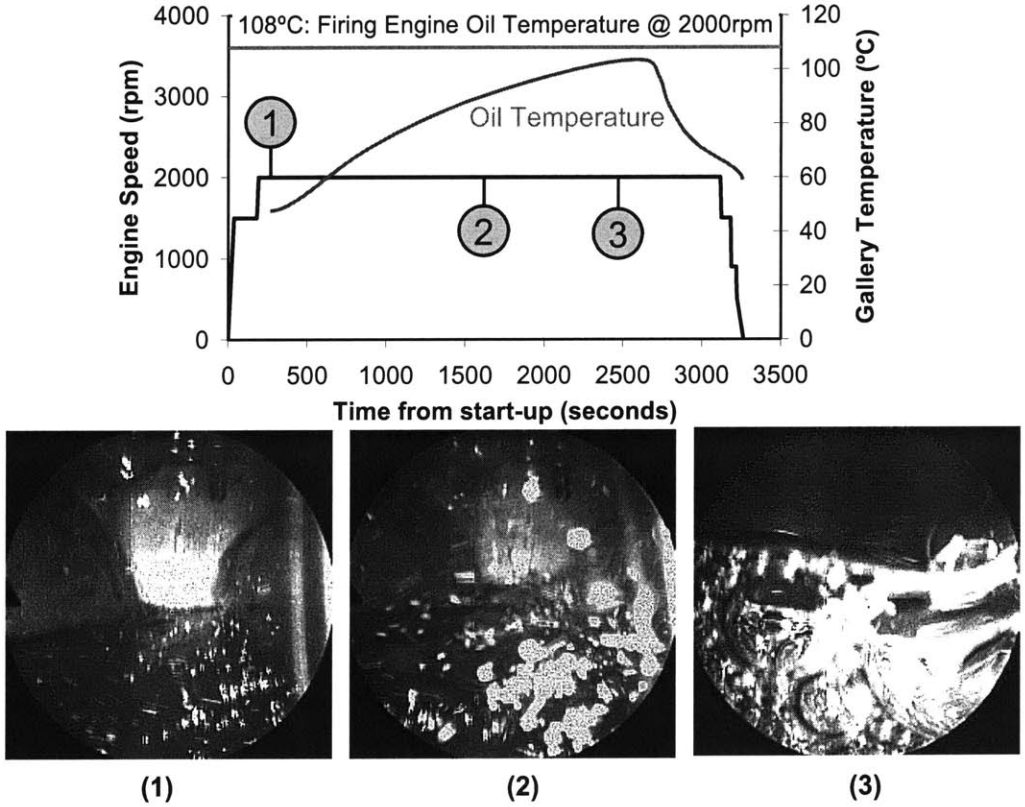

Figure 3-17. Foam formation at a constant engine speed (windage tray and 4L of oil)

The threshold for foam formation is also highly temperature dependent. Therefore the speed threshold above which foam is formed is also highly temperature dependent.

Foam formation was observed when the modified windage tray was installed. Shown in Figure 3-18, the oil droplets were seen above the oil surface, while air bubbles moved along the surface. In the first image, air bubbles were seen below the oil surface and proceeded to break the free surface of the oil and formed a foam network. This network was sustained, even as the speed decreased from 2500rpm to 2000rpm. Though engine speed is critical to foam formation, the formation and destruction mechanisms of foam are highly complex.

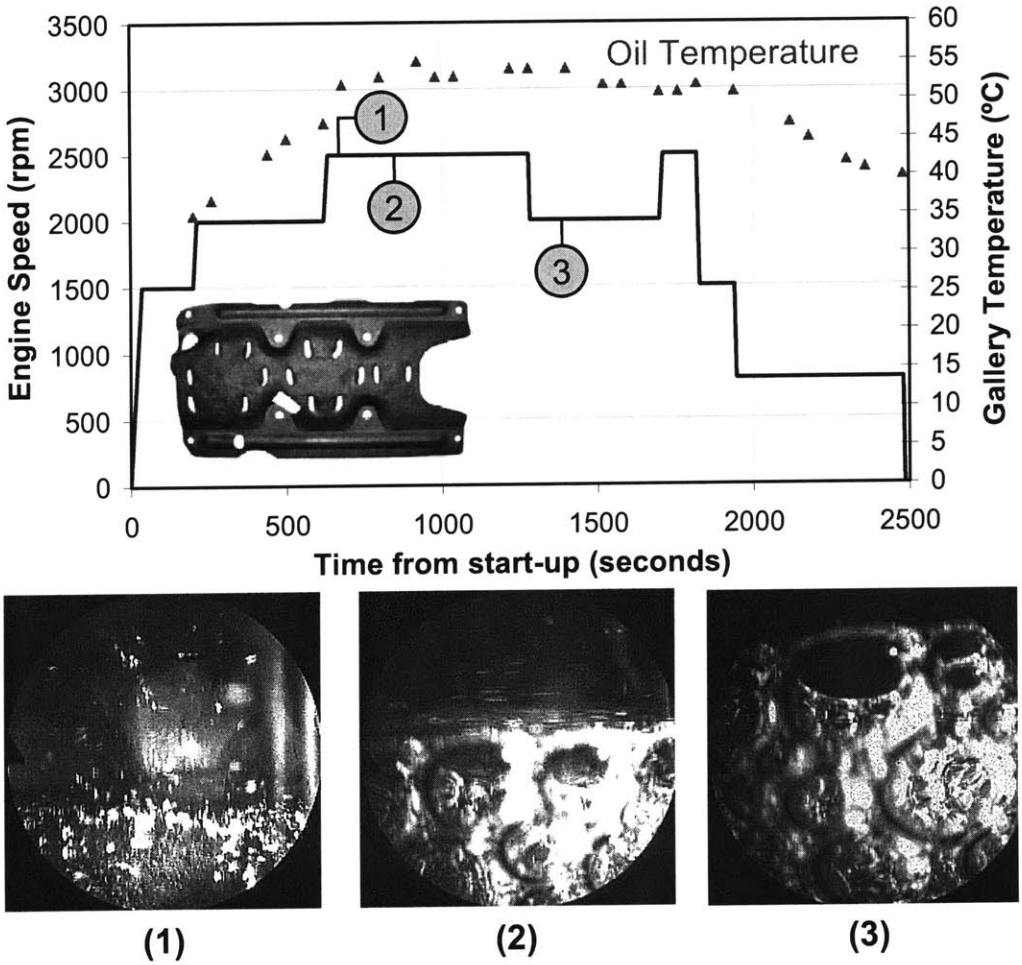

Figure 3-18. Foam formation (modified windage tray and 4L of oil)

When the windage tray was removed, no foam was visually observed (up to an engine speed of 4000rpm and over the same low oil temperature operating conditions). When experiments were performed with the windage tray, many of the droplets departing the crankshaft were shielded by the windage tray and were unable to strike the foam. When the surface foam and bubbles just beneath the surface were exposed to the high-speed droplets, bubble destruction was observed. If the rate of bubble destruction was higher than the rate of bubble formation, no foam was formed.

3.2.5 Experiments on a Firing Engine

Firing engine aeration experiments were performed at Roush Industries in Livonia, MI. Prior to testing, Roush Industries fabricated a camera stand to accommodate mounting. To avoid removing and re-mounting the exhaust manifolds, the oil pan was modified to ensure the camera did not come into contact with the exhaust.

Prior to experimentation, 4.7L (5 qt) of new Shell 5W-20 GF4 oil was added to the engine. The motored visualization experiments at MIT used anywhere between four and five liters of Motorcraft 5W-20. Once the set-up was complete, the engine was spun up to 650rpm. After 10 minutes, the engine speed was increased to 2000rpm and data acquisition commenced. The engine operating sequence, viewing direction and an example image at 2000rpm is shown in Figure 3-19. It should be noted that zero on the time axis corresponds to the commencement of data acquisition and not engine start-up.

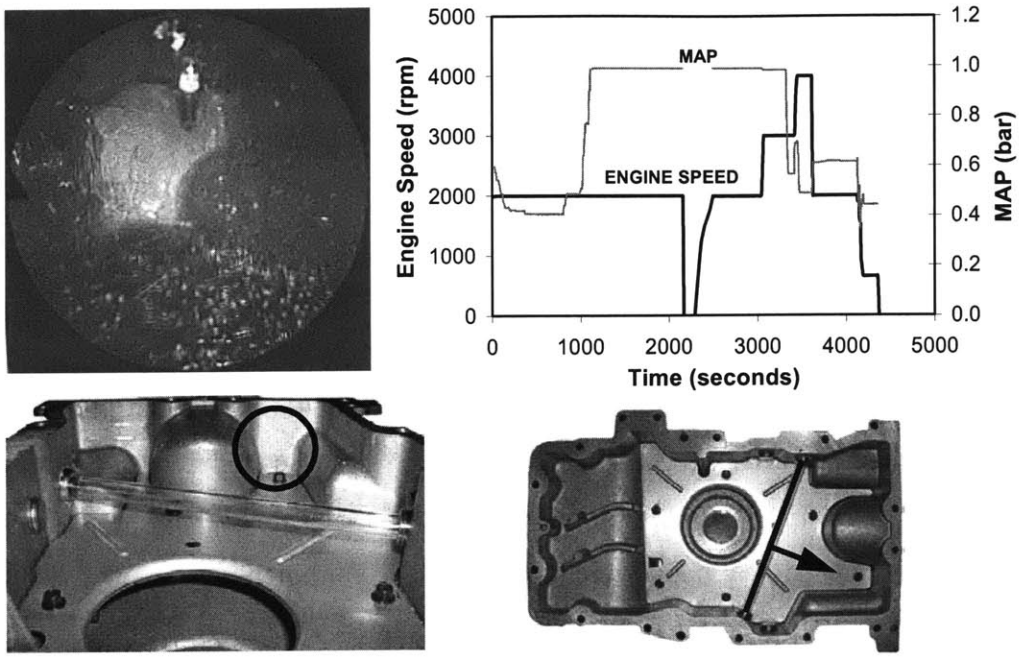

Figure 3-19. Engine operating sequence and viewing direction

During the first 1000s, the intake pressure (MAP) was approximately 0.5bar. After 1000s, the intake pressure increased to full load (1.0bar). At approximately 2100s, the coolant temperature exceeded 102°C (the coolant temperature threshold in the engine control program) and the engine shut down. Soon after, the engine was re-started and testing resumed.

Prior to data acquisition, bubbles were observed on the surface of the oil, and oil drain back could be seen in the rear, left corner of the oil pan. In the first 1000s of data acquisition, the engine load was reduced and the water control valve on the Modine oil cooler was opened. This caused the oil temperature to decrease. In the first 300 seconds, the oil droplet dynamics, oil drain back, and bubble motion on the surface appeared similar to the earlier motored experiments. At 600s, a video of the oil flow through a passage in the windage tray was captured. In this video, oil drain back was observed through a gap in the tray and pulsations of oil emerged from above the tray at the same frequency as the engine speed. Videos were also obtained at full load (1.0bar). The droplet dynamics appeared similar to the half-load operating conditions. It should be noted that the oil temperature was 30°C greater for the full load condition as compared to the half load condition.

Prior to testing at Roush, motoring experiments were performed at MIT. The motoring experiments were performed at an engine speed of 2000rpm and oil temperatures ranging from 30°C to 105°C. As the oil viscosity decreased (temperature increased), the large strings observed at lower oil temperature were no longer present, and instead, the oil draining back into the sump was less ordered.

To ensure videos were obtained at the full range of oil temperatures, the control valve for the Modine oil cooler was shutoff and the engine load was increased to 1.0bar. The oil temperature increased until the cooling water exceeded 215°F (102°C). At this temperature, the engine was shut down and data acquisition halted. Approximately 350s later, the engine was restarted and data acquisition reconvened. Videos were acquired at 2000rpm and appeared qualitatively similar to the videos at 2000rpm, before the engine was shutdown.

As the engine speed increased to 3000rpm, visual access was obstructed due to oil drain back and increased droplet dynamics. After the engine speed increased to 4000rpm, the speed was reduced to 2000rpm, then 650rpm. At this speed, observations of the counterweight through the windage tray passages were made. Prior to the appearance of the counterweight through the windage tray, a negligible number of droplets were observed. When the counterweight appeared, streams of droplets passed through the gap in the windage tray and entered the oil sump (see Figure 3-20).

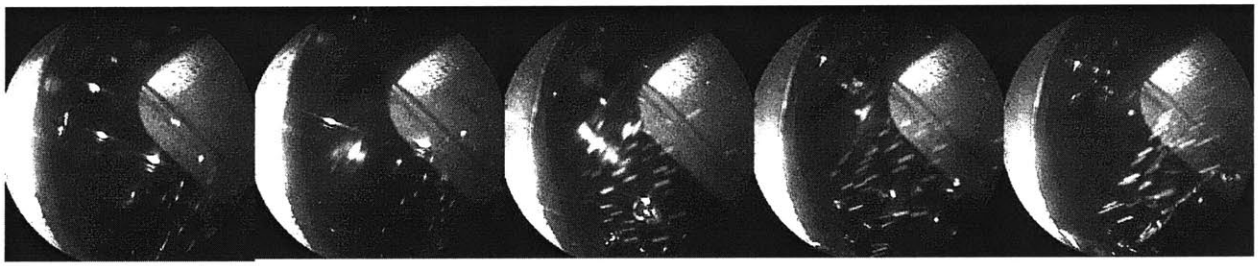

Figure 3-20. Droplets passing through the windage tray of Roush's Ford *Duratec* test engine (left to right: 38ms of video at 650rpm, 0.442bar MAP, and 86.4°C oil temperature).

In this experiment, streams of droplets were flung from the crankshaft, passed through the gaps in the windage tray and struck the free surface of the oil. At engine speeds greater than

3000rpm, visual observation was obstructed. From a qualitative perspective, at the same engine speed and oil temperature, the observations within the oil sump appeared similar in a firing and motoring engine. From the qualitative visual observations in the oil sump, engine load and firing engine operation does not appear to affect the oil aeration in the oil sump.

3.2.6 Engine Shutdown

After the engine was shut down, the oil drained back into the sump and the oil level rose, submerging the borescope. A substantial time was required for the oil to be clear of the air bubbles. The large bubbles rose to the surface much faster than the small bubbles because of buoyancy. Images of the submerged air bubbles at 100s and 500s after the engine shut down are shown in Figure 3-21. Entrained air bubbles were seen rising to the oil surface. At 500s, the total number of air bubbles had decreased substantially and the surviving bubbles were primarily the smaller bubbles.

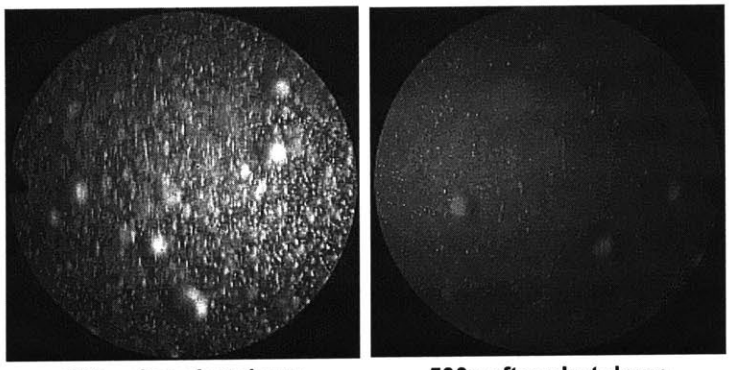

Figure 3-21. After shutdown, entrained air bubbles rose to the surface of the oil (oil temperature of 38°C).

(This page is intentionally blank)

Chapter 4: On-line Measurements of Oil Aeration

Developing a system capable of obtaining a highly accurate, fast response, in-situ oil aeration measurement is a challenging task. Based on an accurate density measurement using x-ray transmission, DSI Deltabeam developed Air-x, a device specifically designed for on-line oil aeration measurements. Many techniques and systems for measuring aeration have already been developed. These aeration measurement techniques are summarized in [27].

4.1 Air-x

Existing ASTM tests related to foaming of lubricating oils (such as D892 and D6082) are laboratory tests that are not representative of oil behavior in an internal combustion engine, where the temperature and pressure are continuously changing along the oil passages [12]. Air-x offers fast response times (less than two seconds) and high accuracy (a tolerance of less than 0.25% aeration). Air-x can be connected anywhere in the engine oil circuit, and is equipped with a qualitative visualization system to observe the oil. The sampled oil volume is small (less than 500mL) and the sampling rate is low (less than 5L/min), to ensure minimal impact on the engine. Air-x is shown in Figure 4-1 connected to the test apparatus.

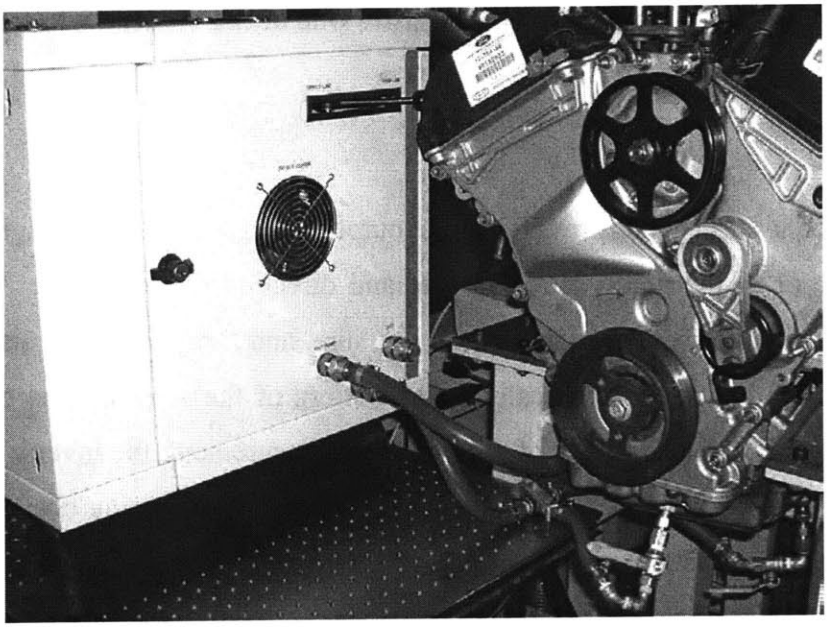

Figure 4-1. Air-X installed on test apparatus

The oil was sampled from three locations in the oil pan. Each location was sampled independently, entered Air-x, and passed through the measuring chamber. In the chamber the oil pressure and temperature were measured, the x-ray measurements were made, and the video capture was performed. After exiting the measuring chamber, the oil entered a pump and was then sent back to the oil pan. A diagram of the measuring chamber is shown in Figure 4-2.

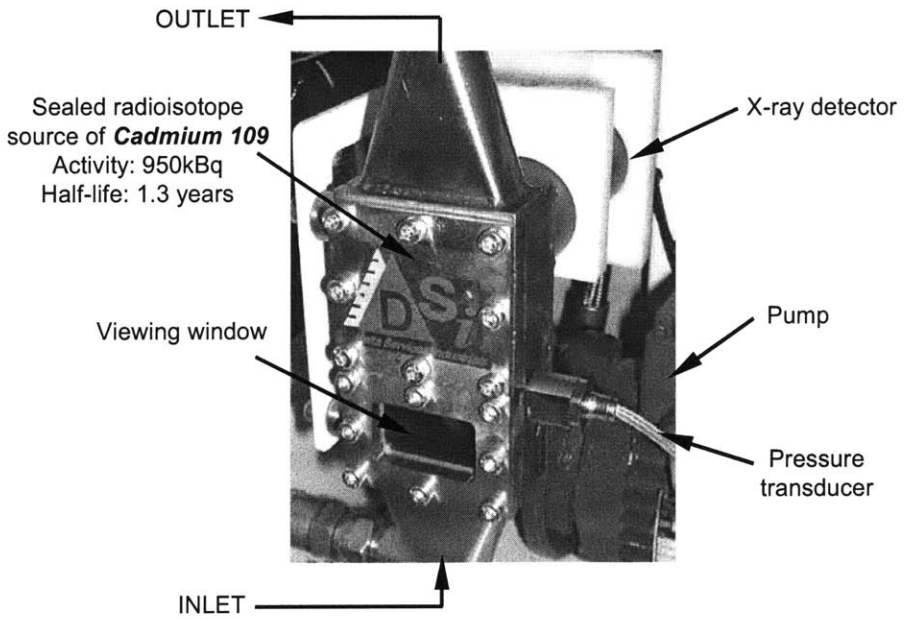

Figure 4-2. Air-x measuring chamber. Thermocouple is located inside the measuring chamber outlet. Camera is located on the opposite side of the viewing window.

4.1.1 Interface

The Air-x interface was set-up to provide engine output parameters such as engine speed, while allowing full control of the pump sampling rate and direction of flow. The Air-x outputs of aeration, corrected aeration, oil temperature, oil pressure, and x-ray yield are displayed for each measurement ID and displayed graphically at the bottom of the screen. The measurement ID number and the dwell time (the length of time of each measurement: the inverse of the sampling frequency) are also displayed. A camera situated beneath the measuring chamber captures the flow through Air-x. The interface is shown Figure 4-3.

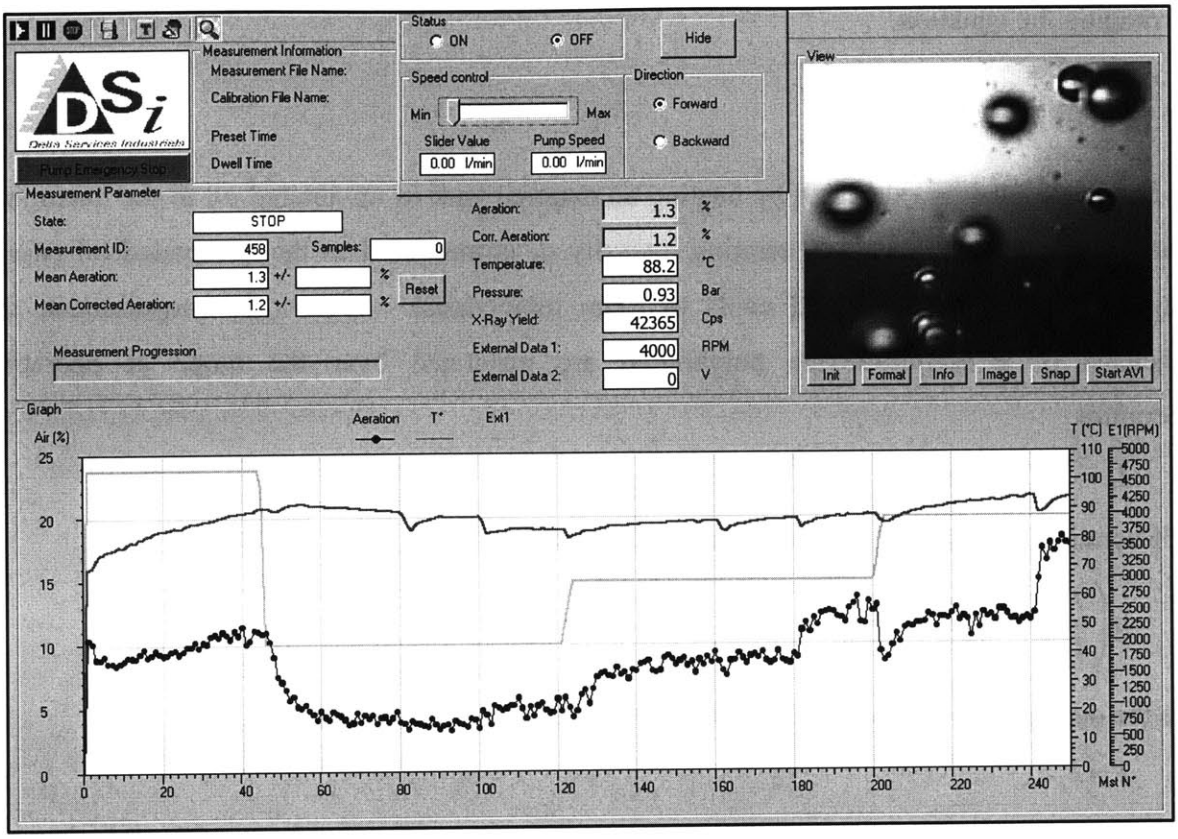

Figure 4-3. DSI Deltabeam - Air-x software interface

4.1.2 Operating Principle

When a low energy x-ray passes through the sampled oil, x-rays are absorbed via the photoelectric and Compton effects. The amount of absorbed x-ray is dependent on the x-ray energy, the thickness and density of the crossed material, and the material composition [12]. The loss of intensity of an x-ray beam is given by:

$$I = I_o e^{-\mu\rho\chi}.$$

Where I is the intensity of the transmitted beam (number of x-rays per second),

I_o is the intensity of the source beam (number of x-rays per second),

μ is the absorption coefficient, which depends on x-ray energy and material (cm^2/g),

ρ is the density of the crossed material (g/cm^3), and

χ is the thickness of the crossed material (cm).

Re-arranging the equation,

$$\ln\left(\frac{I}{I_o}\right) = -\mu\rho\chi .$$

As a first step, Air-x is calibrated by heating an external tank of un-aerated oil to the maximum operating temperature. The 0% aeration intensity, I_1 is measured as the un-aerated oil passes through measuring chamber and cools to room temperature. From this measurement, the coefficients of a second-degree polynomial are generated over the range of operating temperature.

$$I_1 = AT^2 + BT + C .$$

At 0% aeration, the intensity of the transmitted beam is given by,

$$\ln\left(\frac{I_1}{I_o}\right) = -\mu\rho\chi .$$

Since the density at 100% aeration (no oil in the measuring chamber) is negligible,

$$I = I_o .$$

Since the x-ray measurements are performed after the 0% aeration has been calibrated, they are corrected by the decay of Cadmium 109 radioisotope source.

$$I_m = Ie^{\frac{-t}{T_{1/2}}\ln(2)} .$$

If aeration is defined as the ratio of the density of the mixture to the un-aerated oil,

$$\phi = \frac{V_{air}}{V_{air} + V_{oil}} 1 - \frac{\rho}{\rho_1} = 1 - \frac{\ln(I_m) - \ln(I_o)}{\ln(I_1) - \ln(I_o)} .$$

Since the distance the oil travels through Air-x (from the sump to the measuring chamber and back to the sump) is relatively short (less than 1m), no temperature correction was made. However, since the pump is located downstream of the measuring chamber, the pressure is the measuring chamber is less than one atmosphere. When the pressure decreases from the ambient pressure, the entrained air expands according to Boyle's Law and the dissolved air transforms into entrained air according to Henry-Dalton's Law. Thus the total air volume is exaggerated in the measuring chamber and must be accounted for in the aeration calculation. The x-ray measurement is shown schematically in Figure 4-4. The specifications are shown in Table 4-1.

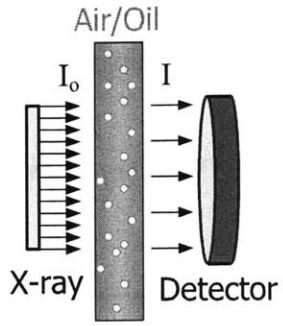

Figure 4-4. Schematic of x-ray absorption in Air-x

Table 4-1. Air-x specifications

Dimensions (W x H x D)	600mm x 520mm x 483mm
Mass	50kg
Viscosity range	3.8mm^2/s to 3500mm^2/s
Temperature range	0 to 150°C
Pressure range	0 to 10bar
Oil flow	0 to 5L/min
Measurement range	0 to 100% aeration
Accuracy	At 10s acquisition time: 0.5% At 100s acquisition time: 0.2%
Sample oil volume	less than 500mL
Aeration data	0% of oil aeration: 0V 100% of oil aeration: 4V

4.1.3 Calibration

Since the density is critical to the calculation of thickness of the crossed material, it is important to determine the engine oil density as a function of temperature. To determine the density of the oil over the operating temperature range, Air-x is connected to a tank, where the oil is heated to 110°C. The Air-x pump circulates the oil through the apparatus, and x-ray absorption measurements are made as the oil cools to 20°C. During this process, it is critical that no oil aeration occurs, and this is validated with the Air-x camera. From the measured x-ray transmission at 0% aeration, the oil density as a function of the temperature can be determined.

$$\rho(T) = -\frac{1}{\mu\chi}\ln\left(\frac{I(T)}{I_o}\right).$$

Where $\rho(T)$ is the engine oil density at temperature T, and

$I(T)$ is the intensity of x-rays crossing the engine oil at temperature, T.

The x-ray yield and density for Motorcraft 5W20 are shown in Figure 4-5.

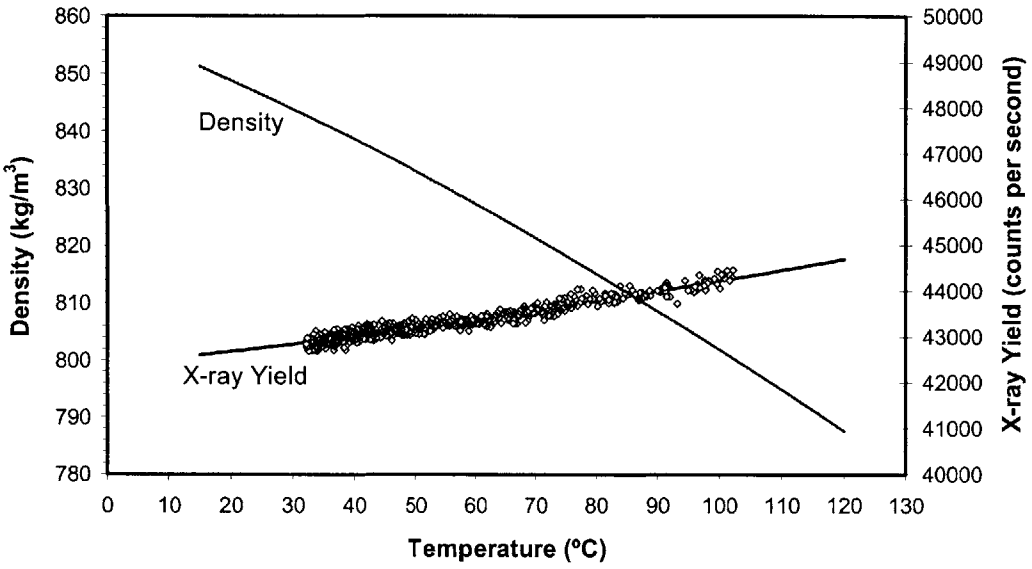

Figure 4-5. Motorcraft 5W-20 density and x-ray yield over the range of operating temperatures

To determine the aeration standard, the limiting aeration conditions are used. The x-ray transmissions at 0% air (chamber filled with engine oil) and 100% air (chamber filled with air) are used to create the calibration curve for the engine oil.

4.1.4 Measurement Locations

The oil pan was modified to allow for three sample locations: Location # 3 samples the sump oil near the baffle, approximately 10mm below the oil surface (though this depends on the oil volume added to the engine). Location # 1 samples the oil near the pick-up tube, and Location # 2 samples the head return oil that collects in a 100mL container (see Figure 4-6). In addition, oil is returned to the sump at Location # 4, the borescope tube passage is shown at Location # 6, and the sight glass in the bottom of the oil pan is shown at Location # 5.

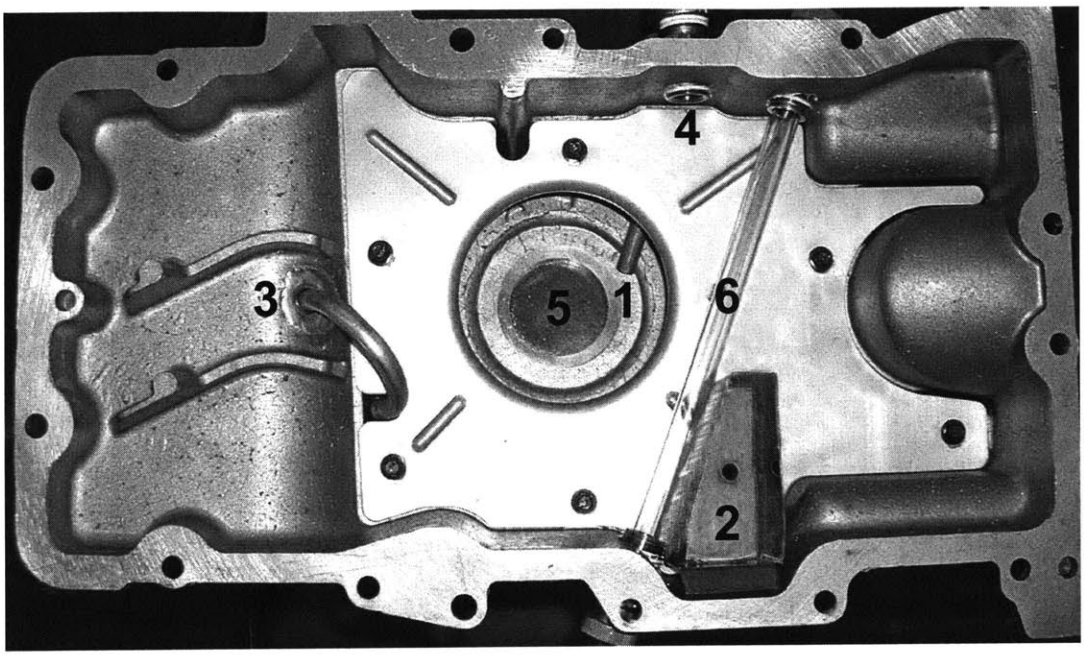

Figure 4-6. Oil pan modifications: (1) Pick-up sample location, (2) head return sample location, (3) sump sample location, (4) Air-x return location, (5) sight glass, and (6) borescope tube passage

Sampling at Location # 1 provided an estimate of the oil aeration entering the pick-up tube. At Location # 3, oil was sampled from below the oil surface. Since the return oil from the left head enters the oil sump at Location # 2, the oil fills the container and a continuous aeration measurement can be made. All of the sampled oil returns to the oil pan from Air-x at Location # 4. From these three oil samples, aeration measurements of the head return oil, oil entering the pick-up, and the surface of the oil in the sump can be compared and the air transport mechanisms can be deduced. In conjunction with prior video observations, these aeration measurement comparisons will highlight the contributions of various sources to oil aeration. An external view of the plumbing is shown in Figure 4-7.

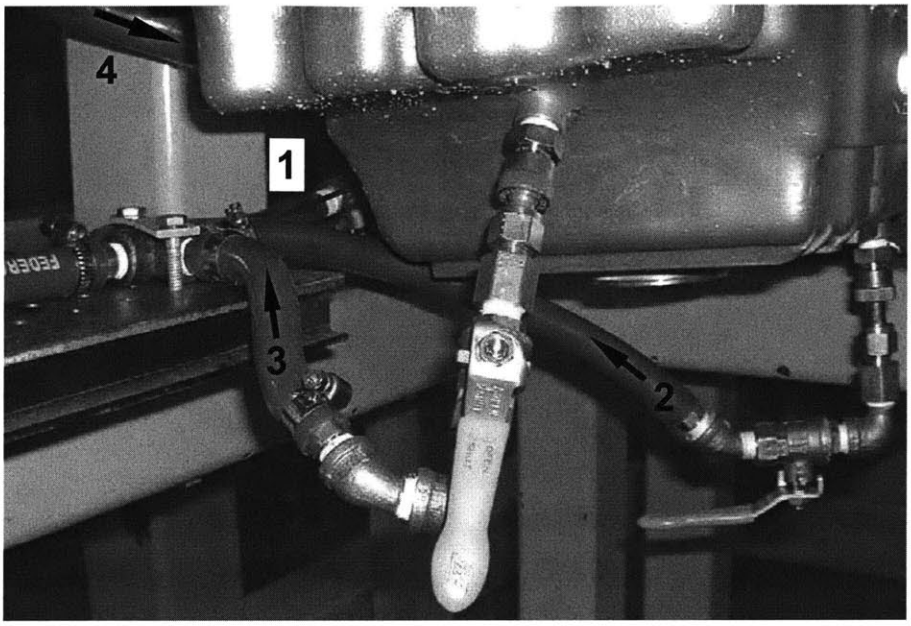

Figure 4-7. External Air-x plumbing. Note that the valves were replaced with pneumatically actuated valve, and labeling corresponds with the internal sample locations shown in Figure 4-6.

4.1.5 Corrections

Based on conservation of mass, the number of moles of air (including both entrained and dissolved air) in the oil sump sample is equivalent to the number of moles of air in the measuring chamber (see Figure 4-8).

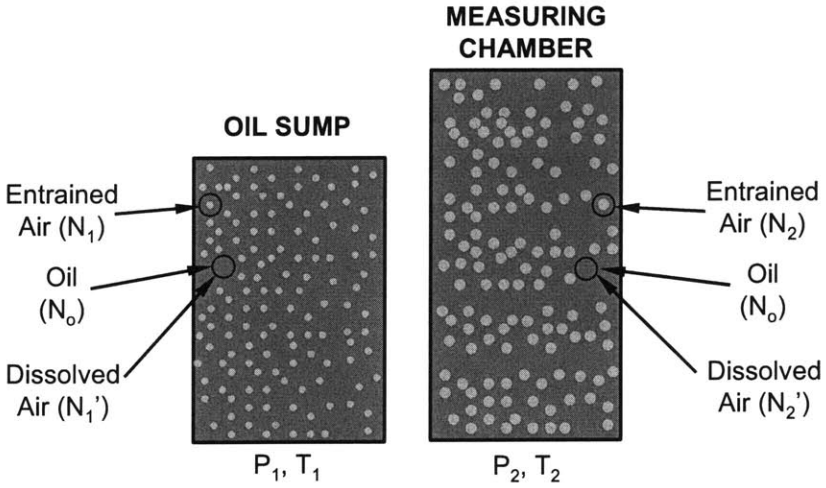

Figure 4-8. Oil sampled from the sump and measured in the measuring chamber

This can be written as,

$$N_1 + N_1^{'} = N_2 + N_2^{'}.$$

According to Henry-Dalton's Law (see Chapter 1 for description),

$$\left(\frac{V_1^{'}}{V_o}\right)_{ref} = B_1 P_1, \text{ and } \left(\frac{V_2^{'}}{V_o}\right)_{ref} = B_2 P_2.$$

Where, the volume of dissolved air and the volume of oil are defined at 20°C and atmospheric pressure. In general, the Bunsen coefficient, B decreases with increasing temperature. However, for engine oils the Bunsen coefficient is approximately 9%/bar [16], and essentially constant over the range of oil temperatures encountered in an engine [6]. Since the engine oil temperature is much greater than the reference temperature, a temperature correction must be considered. Assuming that the oil volume varies only moderately from 20°C to 140°C and air behaves as an ideal gas,

$$\left(\frac{V_1^{'}}{V_o}\right)_{ref}\left(\frac{T_1}{T_{ref}}\right) = \frac{V_1^{'}}{V_o}, \text{ and } \left(\frac{V_2^{'}}{V_o}\right)_{ref}\left(\frac{T_2}{T_{ref}}\right) = \frac{V_2^{'}}{V_o}.$$

The conservation of mass equation becomes,

$$\frac{P_1 V_1}{RT_1} + \frac{P_1 V_1^{'}}{RT_1} = \frac{P_2 V_2}{RT_2} + \frac{P_2 V_2^{'}}{RT_2}.$$

Combining Henry-Dalton's Law with the conservation of mass,

$$\frac{P_1 V_1}{RT_1} + \frac{V_o B_1 (P_1)^2}{RT_{ref}} = \frac{P_2 V_2}{RT_2} + \frac{V_o B_2 (P_2)^2}{RT_{ref}}.$$

Air-x measures the aeration, ϕ as the volume of air (entrained) to the volume of mixture (entrained air and oil).

$$\phi_1 = \frac{V_1}{V_1 + N_o / \rho_{M1}}, \text{ and } \phi_1 = \frac{V_2}{V_2 + N_o / \rho_{M2}},$$

Where, ρ_M is defined as the molar oil density (kmol/m^3).

$$\rho_M = \frac{N_o}{V_o}.$$

Isolating the volume of air,

$$V_1 = \frac{N_o / \rho_{M1}}{1/\phi_1 - 1}, \text{ and } V_2 = \frac{N_o / \rho_{M2}}{1/\phi_2 - 1}.$$

Re-writing the conservation of mass equation, where the unknown is ϕ_1,

$$P_1\left[\frac{\frac{N_o/\rho_{M1}}{1/\phi_1-1}}{RT_1}+\frac{N_oB_1P_1}{\rho_{M1}RT_{ref}}\right]=P_2\left[\frac{\frac{N_o/\rho_{M2}}{1/\phi_2-1}}{RT_2}+\frac{N_oB_2P_2}{\rho_{M2}RT_{ref}}\right].$$

Since the sampling tube length is less than 1m, the temperature of the oil decreases only minimally from the sump to the measuring chamber. Therefore, it was assumed that the temperature in the measuring chamber (T_2) was equivalent to the temperature in the sump (T_1). This is an excellent approximation as the temperature of the oil sample in the measuring chamber was within 4°C from the measured oil block temperature. This was observed during all experiments with an oil temperature between 80°C and 110°C, independent of engine speed. The density of the oil was calculated from the density-temperature relationship obtained during the 0% aeration calibration. The measuring chamber pressure (P_1) was measured, and the sump pressure was assumed to be constant at 1atm. For all three sample locations the measuring chamber pressure remained greater than 0.8bar, when the sampling rate was 1L/min, over a temperature range from 80°C to 100°C. Six consecutive measuring chamber temperature and pressure measurements (two at each of the three sample locations) are shown in Figure 4-9.

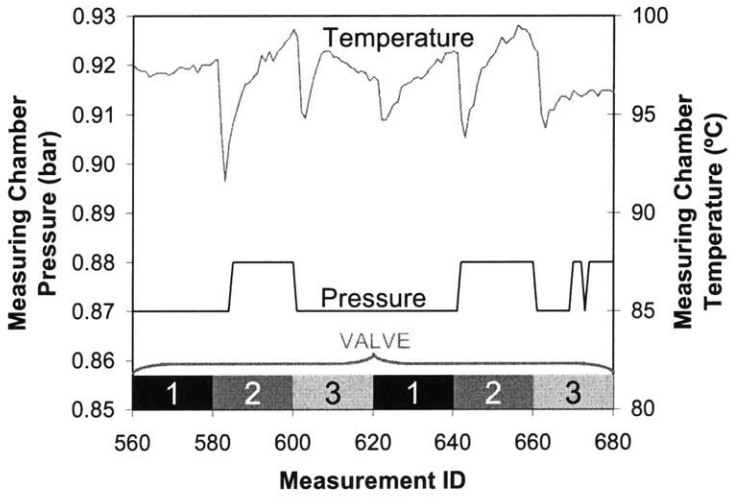

Figure 4-9. Measuring chamber temperature and pressure for each of the three sample locations. Experiment performed at 4000rpm, 5s per measurement ID, with the windage tray.

This figure suggests that the pressure drop between the oil sump and the measuring chamber is comparable for each of the three sample paths. The oil flow diagram for each sample location is shown in Figure 4-10.

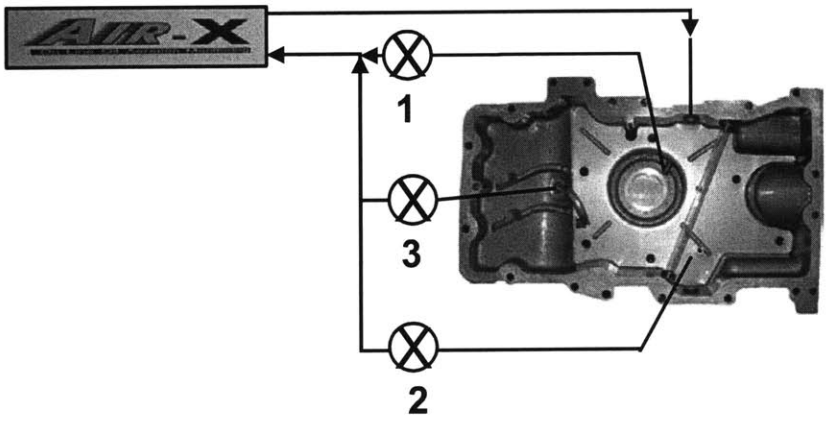

Figure 4-10. Schematic of the oil flow path from the oil sump (location 1, 2 or 3) to Air-x and returning to the oil sump

Since there was only a moderate pressure drop between the oil sump and measuring chamber, minimal dissolved air transformed into entrained air. Deconninck *et al.* used Air-x to predict the dissolved air released from the air-oil mixture by placing a flow restriction upstream of Air-x [12]. The pressure drop generated entrained air from the dissolved. At 0.8bar, only 2.4% of dissolved air was released in a fluid with a Bunsen Coefficient of 12%/bar. Since the pressure in the measuring chamber is greater than 0.8bar and the engine oil Bunsen Coefficient is less than 12%, the dissolved air generated from the pressure decrease is less significant. It was also observed that the Bunsen Coefficient does not significantly affect the corrected aeration measurement for the experimental operating conditions. For a 5% aeration measurement in the measuring chamber, the corrected aeration (aeration in the oil sump) is shown in Figure 4-11 over a range of measuring chamber pressures and oil Bunsen Coefficients.

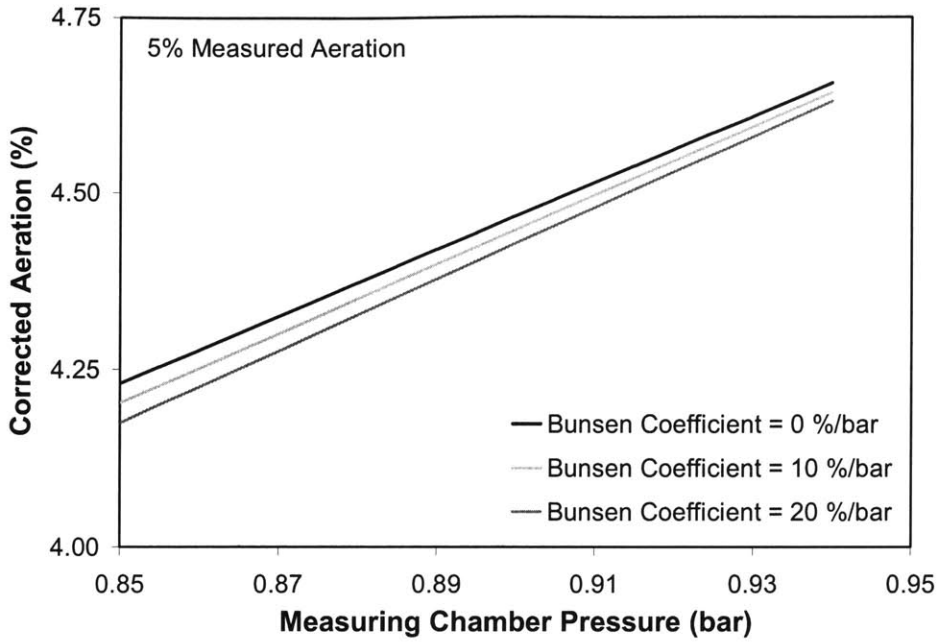

Figure 4-11. Corrected aeration for a 5% aeration measurement over a range of Bunsen Coefficients and measuring chamber pressures

Deviating from the commonly accepted engine oil Bunsen Coefficient of 9%/bar will only moderately influence the aeration correction. As such, 9%/bar was used throughout this study. Air-x measures the aeration in the measuring chamber (ϕ_2). From all of these measured and assumed values, the corrected aeration (ϕ_1), the aeration in the oil sump, is calculated.

$$\frac{\phi_1}{1-\phi_1} = \underbrace{\left\{\frac{P_2}{P_1}\frac{\phi_2}{(1-\phi_2)}\right\}}_{\text{Density of gas correction}} + \underbrace{B\left(\frac{T}{T_{ref}}\right)\left(\frac{P_2^{\,2}-P_1^{\,2}}{P_1}\right)}_{\text{Desorption / Absorption correction}}.$$

In the following discussion, the term "aeration" refers to the corrected aeration calculated as described above.

4.1.6 Aeration Measurements

Once a 0% and 100% aeration calibration have been performed, the experiment time scale must be specified. The averaging time scale is the length of time over which x-rays are counted. Since most measurements were taken at a single operating condition for more than 100s, a 5s

averaging cycle was chosen. This time scale allowed for 20 aeration measurements over the 100s sample period.

Experiments were performed over a range of oil temperatures from 20 to 110°C and engine speeds from 0 to 6000rpm. Experiments were also performed with and without the windage tray. A sample aeration measurement is shown in Figure 4-12. The x-ray count was averaged over a 5s interval, and thus the sampling rate was 0.2Hz. Although Air-x is capable of a 1Hz sampling rate, a 0.2Hz sampling rate was sufficient for the times scales of this experiment (at least 100s per sample location).

The sample locations were cycled through in the order of Locations # 1 (near the oil pick-up), # 2 (near the head oil return), and # 3 (near the oil surface). When the engine speed was changed a certain period of time was necessary before a relatively steady aeration measurement was achieved. During experimentation, 20 data points were collected at each sample location. The first 15s (3 data points) were neglected due to the transients in the flow caused by switching the sample location. If the engine speed was changed, either 50s (10 measurements) or 100s (20 measurements) were allowed for transient adjustment.

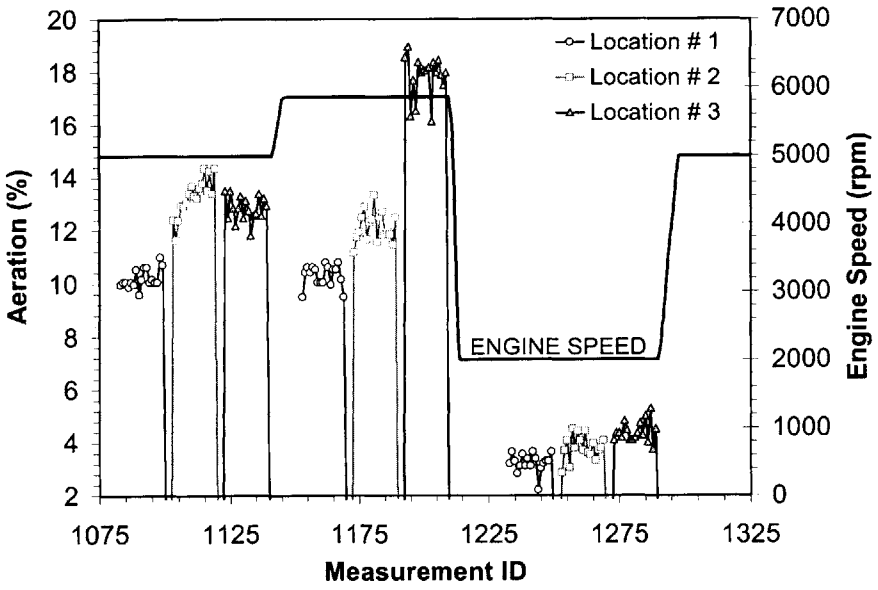

Figure 4-12. Sample aeration measurement cycling between Locations # 1 (near the oil pick-up), # 2 (near the head oil return), and # 3 (near the oil surface). Pump sampling rate of 1 L/min at an oil temperature between 85 and 105°C.

A second parameter of operation is the sampling rate, which is the oil flow through the pump. An aeration sensitivity study was performed to evaluate the influence of the sampling rate on aeration.

4.2 Air-x Sampling Rate

The oil sampling rate is an Air-x input that can be varied from experiment to experiment. A sensitivity study was performed to determine the relationship between aeration and sampling rate. Since the oil pump is located downstream of the measuring chamber and discharges the oil back into a near atmospheric oil sump, as the oil flowrate increases the measuring chamber pressure must decrease to accommodate the increased flowrate. Since the measuring chamber pressure decreases as the oil flowrate increases, more dissolved air was transformed to entrained air in the measuring chamber than at a lower oil flowrate, where only a slightly below atmospheric pressure is required to generate the lower oil flowrate. After the correction described in an earlier section was implemented, the dependence of aeration on sampling rate was observed and is shown in Figure 4-13.

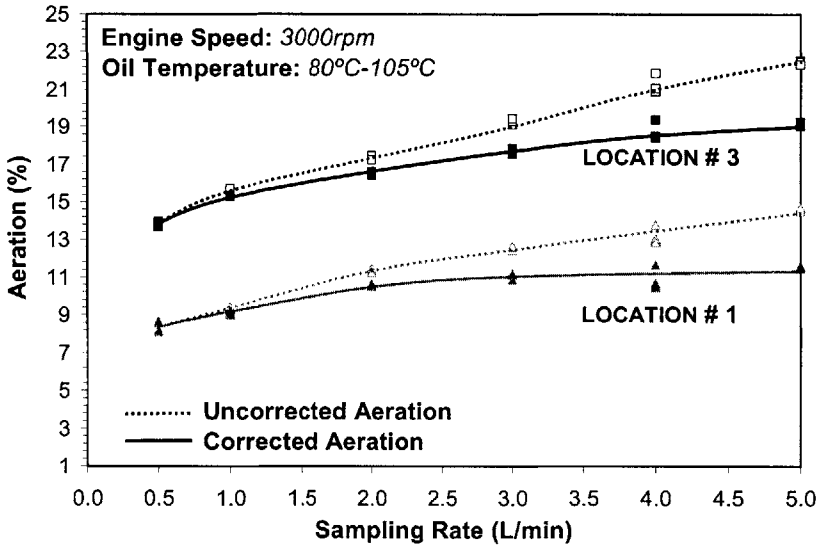

Figure 4-13. Aeration at Locations # 1 (near oil pick-up) and # 3 (near oil surface) over the entire range of oil sampling rates at 3000rpm and steady temperature operation conditions with the windage tray.

The corrected aeration is much less dependent on the sampling rate as compared to the uncorrected aeration. To ensure that air was not drawn into the measuring chamber an oil flow rate of 1L/min was chosen for all experiments. This flow rate was sufficiently high to ensure that a sufficient volume of oil was obtained at each of the locations. It should be noted that Location # 2 (near the oil head return) was not shown in Figure 4-13. The challenges of measuring the head return oil aeration will be discussed in the following section.

4.2.1 Head Return Oil Sampling Methods

In contrast to Locations # 1 and # 3, Location # 2 sampled the oil from a container situated beneath the right head return. The objective of this location was to determine the aeration of the oil returning from head. However, sampling from a container continuously filling with return oil was a difficult task. When the oil is sampled from a container and a gradient in air bubble concentration exists in that container, the aeration measurements is strongly dependent on the oil volume in that container. In this section the engine oil volume was 4L. This was done to match the visualization experiments described in Chapter 3. As shown in Figure 4-14, sampling from this container showed a much stronger dependence on the oil sampling rate. As such, four methods of measuring the aeration at Location # 2 were considered.

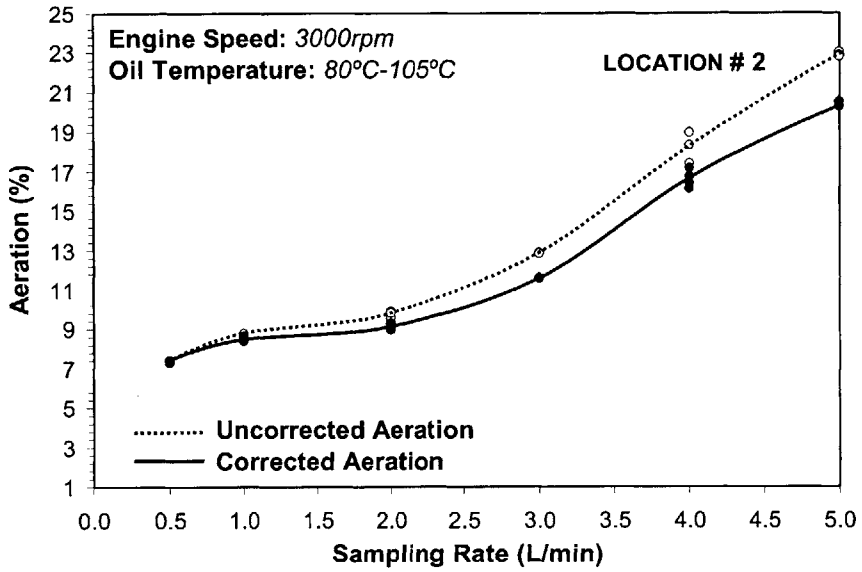

Figure 4-14. Aeration at Location # 2 over the entire range of oil sampling rates at 3000rpm and steady temperature operating conditions.

4.2.1.1 Method 1: Constant Oil Volume

Predicting the "optimum" sampling rate is a complicated matter since the rate of oil entering the container is difficult to measure. With the aid of the high-speed camera, the oil entering the container from the left head was observed. The sampling rate was adjusted to ensure that no oil returning from the head would spill over the container. If the oil spilled over the container, the sampling rate was increased until overflow was not observed. It was clear that the amount of oil returning from the head was dependent on the oil temperature because as the oil temperature increased it was necessary to sample at a higher rate to ensure no oil overflowed. Since visual observation was only available at engine speeds below 4000rpm, the head return oil flowing into the container was predicted over a range of oil operating temperatures at engine speeds below 4000rpm. By ensuring that the no oil spilled over the container and no air was drawn into the sampling location at the bottom of the container, a comparative aeration measurement was obtained over a range of engine speeds. The two limiting cases are shown schematically in Figure 4-15.

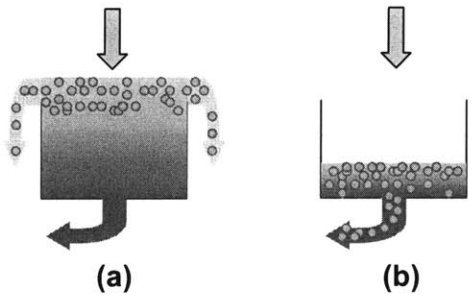

Figure 4-15. (a) Oil spilling over the container (sampling rate less than the rate of oil entering the container), and (b) oil level decreasing in the container (sampling level greater than the rate of oil entering the container).

Using the high-speed video equipment, the oil overflowing the container during engine operation was observed from the viewing tube. Images of an empty and overflowing container are shown in Figure 4-16.

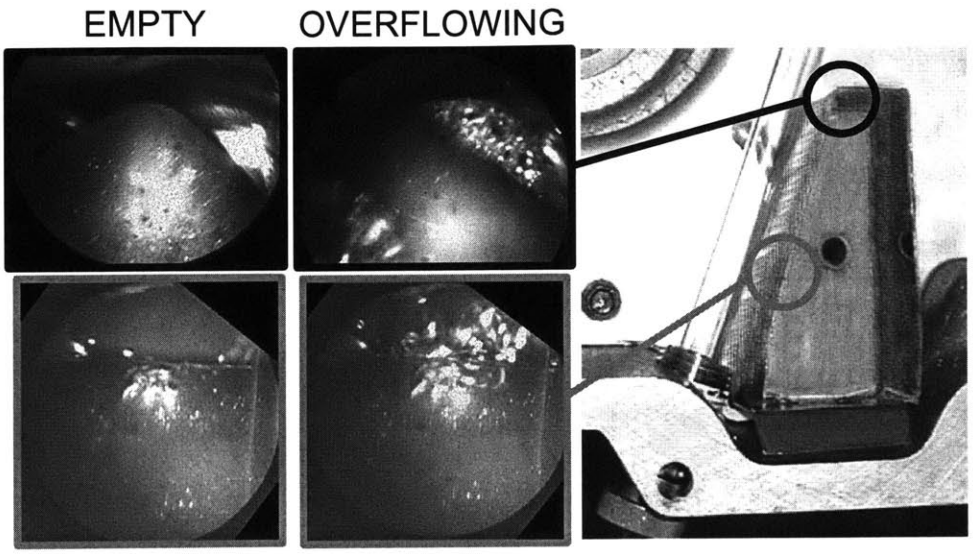

Figure 4-16. Observing the oil exiting the container situated beneath the head oil return

Based on oil temperature and engine speed, a correlation between the oil flowing into the container and the oil temperature was determined at engine speeds between 1000rpm and 3000rpm (see Figure 4-17).

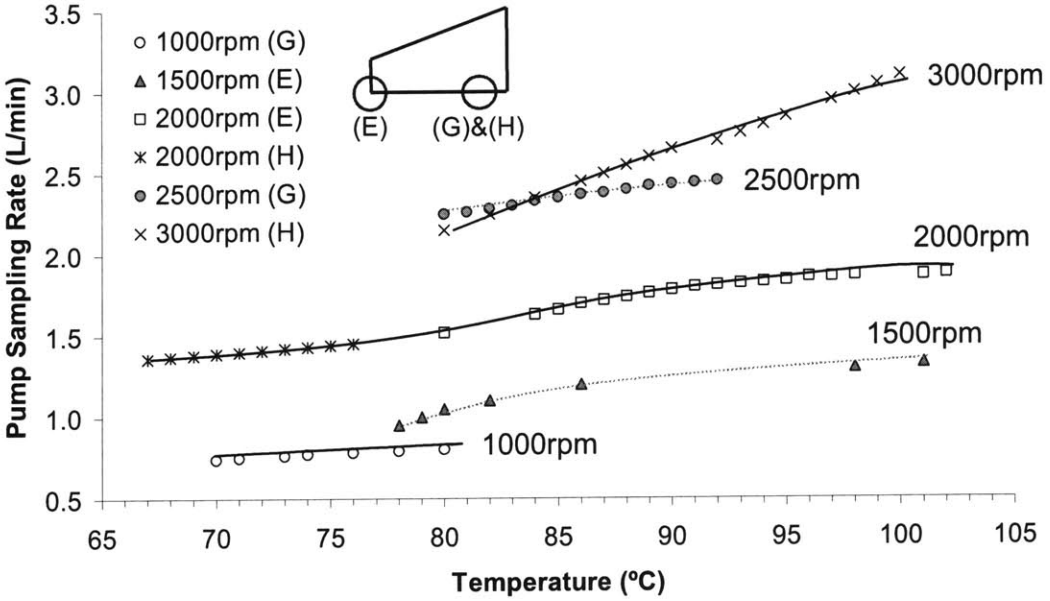

Figure 4-17. Sampling rate to ensure that no oil spilled over the container and the oil level did not decrease in the container. The container location observed during experimentation is shown adjacent to the legend. The letter in brackets refers to the experiment.

From these correlations, an oil sampling rate was specified at a given temperature and engine speed. During the development of these correlations, the aeration was measured and the aeration of the oil in the container increased significantly with engine speed and only moderately with oil temperature (see Figure 4-18).

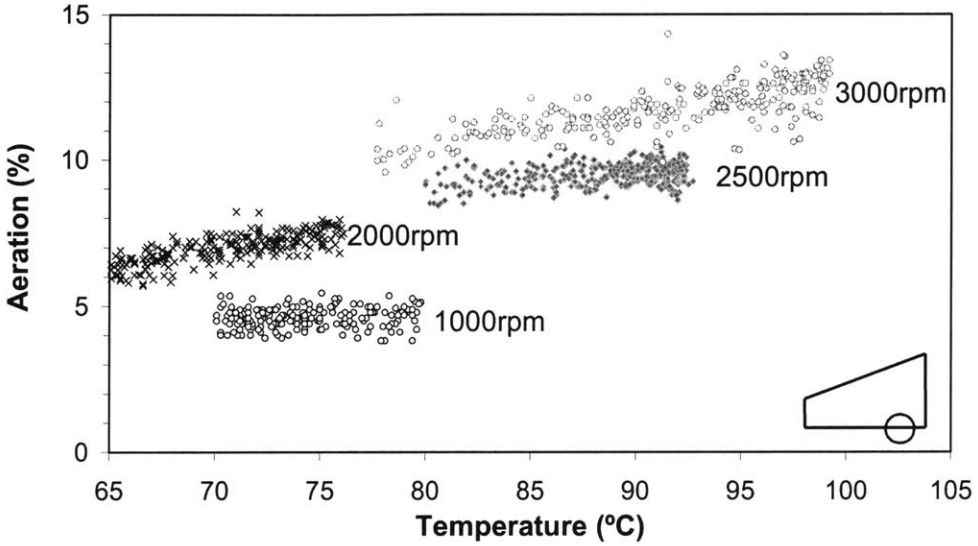

Figure 4-18. Aeration over a range of oil temperatures for one of the two observation locations (location shown in the bottom right corner).

This method of measuring the aeration provided a relative comparison between the aeration of the head return oil as a function of engine speed and oil temperature, however the magnitude of the aeration, in comparison to the other sampling location, is difficult to establish because the oil may partially de-aerate while occupying the container. Even if this problem is addressed it is unclear as to whether or not this technique provides a representative measure of the head return oil aeration.

4.2.1.2 Method 2: Constant Sampling Rate

A more simplistic approach would be to sample the oil from the container at a constant rate, independent of the oil temperature and engine speed. However, this technique has its associated problems. For example, at a low engine speed (lower oil flow rate) and high oil sampling rate the sampling location is starved of oil, which results in air being drawn into Air-x. Alternatively, at a high engine speed (higher oil flow rate) and low oil sampling rate, the oil entering the

container spills over the edge of the container and does not significantly mix with the oil already in the container.

The container resident time is defined as shortest time to remove every oil molecule from the container (assuming perfect mixing). The long container resident time permits air to escape from the oil, which results in an underestimate of the head return oil aeration. A comparison between Method 1 (constant oil volume) and Method 2 (constant sampling rate) is shown in Figure 4-19.

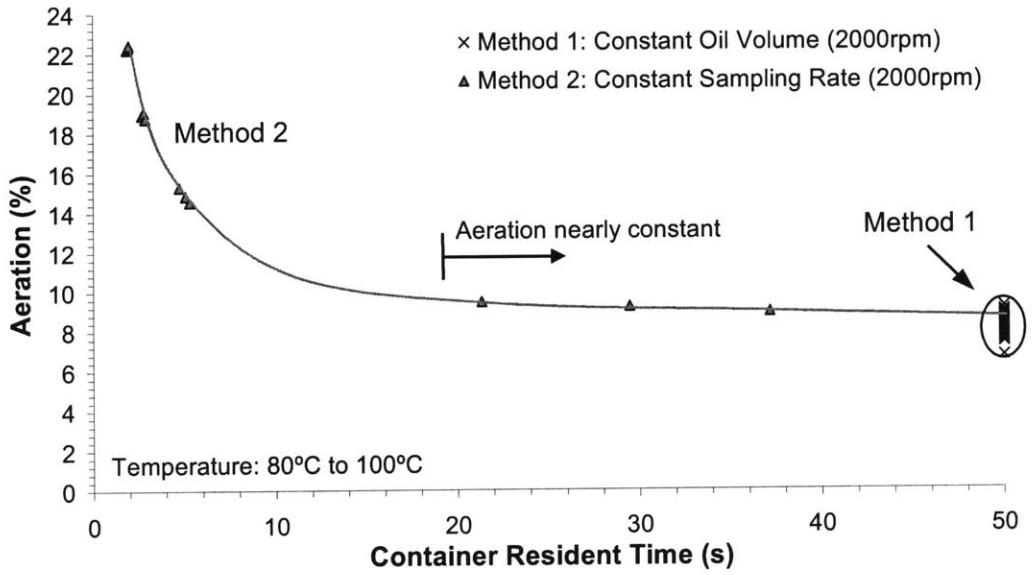

Figure 4-19. Comparing the aeration measurements at 2000rpm using Method 1 (constant oil volume) and Method 2 (constant sampling rate). Container resident time is varied by specifying the sampling rate between 0.5 and 5L/min.

Since the sampling rate for Method 1 (constant oil volume) was adjusted to ensure that no oil spilled over the container the container resident time is much greater than that of Method 1 (shown as 50s in Figure 4-19, however the resident time is likely much longer). Figure 4-19 suggests that at container resident times below 10s (sampling rates greater than 3L/min) air is drawn into Air-x.

The first method of comparing the return oil aeration varied the sampling rate to match the oil flowing from the head return oil into the container. This ensured that no fresh oil overflowed into the sump. However, the first method of comparing the return oil aeration permitted a longer

container resident time for the lower speed, lower temperature operating condition, when the return oil flow into the container was much less. This may lead to some inaccuracies when considering two experiments with different engine speeds. The second method of predicting return oil aeration (constant sampling rate) does not fairly evaluate the aeration over the range of engine operating speeds and temperatures, but before a magnitude of aeration comparison is made between the head return oil, oil pick-up (Location #1), and oil surface (Location # 3), it is critical that the method of predicting the head return oil aeration is considered further.

4.2.1.3 Method 3 & 4: Vertical Surface and Horizontal Surface Measurement

Since the first two methods did not reveal an aeration measurement independent of both sampling rate and engine speed, additional methods were considered. A tube extension was added to the container. It was thought that sampling near the surface of the oil would provide a more representative measure of aeration as compared to measuring at the bottom of the container. A vertical sampling tube extension (Method 3) and bent sampling tube extension (Method 4) are shown in Figure 4-20.

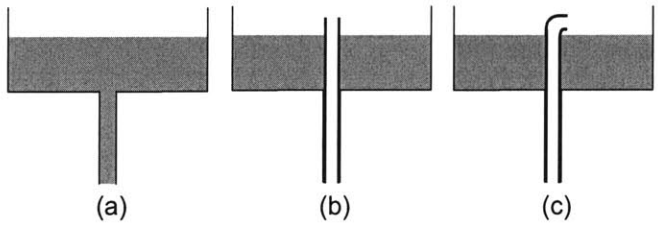

Figure 4-20. Schematic of the container modifications: (a) Method 1 and 2, (b) Method 3 (Vertical Surface Measurement), and (c) Method 4 (Horizontal Surface Measurement).

The container modification for the horizontal surface measurement is shown in Figure 4-21.

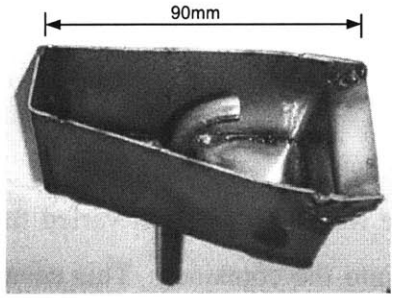

Figure 4-21. Container modification for the horizontal surface measurement

The four methods of measuring the head return oil aeration are shown, over the range of Air-x sampling rates, in Figure 4-22.

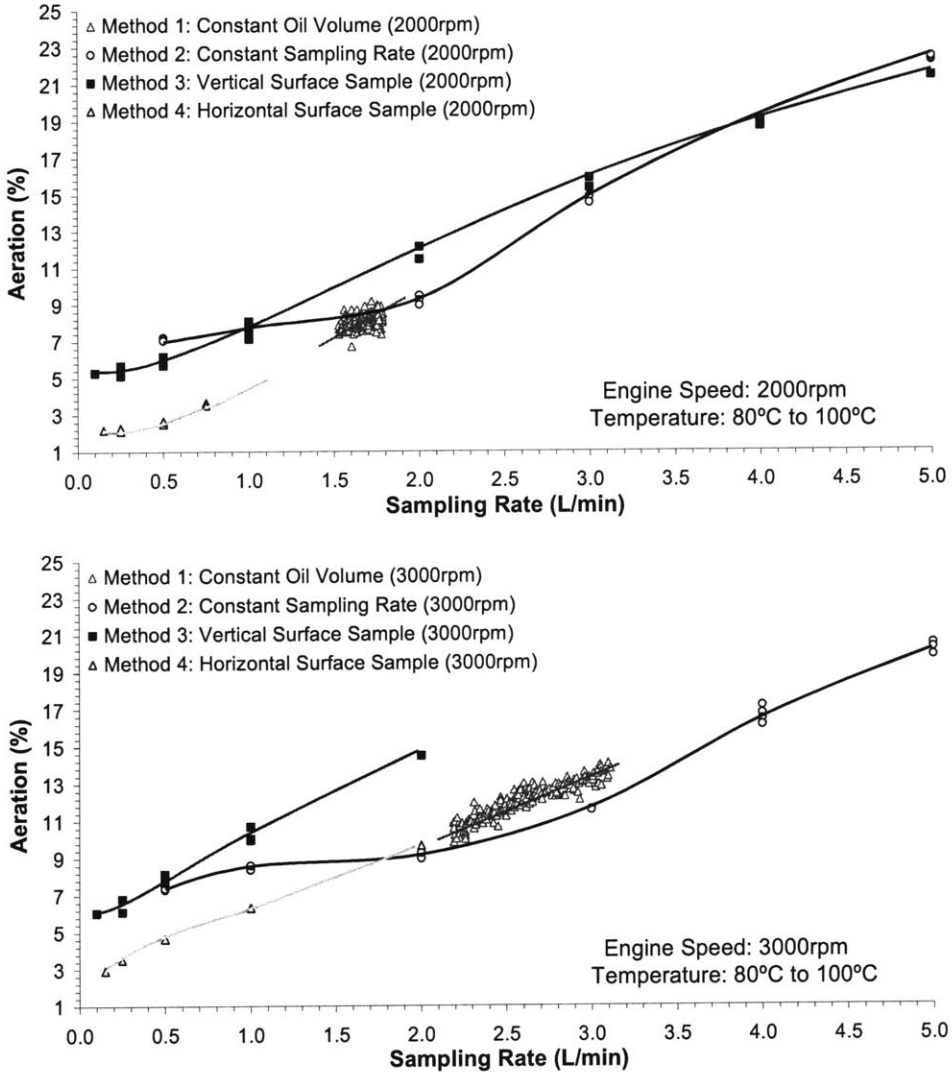

Figure 4-22. Four methods of measuring the head oil return aeration at 2000rpm (top figure) and 3000rpm (bottom figure) at an oil temperature between 80 and 100°C, with the windage tray.

Although the aeration is roughly comparable between these sampling methods, the aeration continues to be dependent on the oil sampling rate. At the high oil sampling rates, Method 3 (Vertical Surface Sample) and Method 2 (Constant Sampling Rate) provide similar results. However, this may be due to air being drawn into Air-x. These four attempts at quantifying the

head oil return aeration highlight the challenges of accurately measuring the contributions of the head oil aeration, experimentally. As such, the container was removed from the oil pan and no further attempts at sampling the return oil via the container were performed.

4.3 Repeatability and Data Analysis

Location # 2 (head oil return) was modified by removing the container from the oil pan and replacing it with a tube that samples the oil above the oil pan baffle, but is located below the left head oil return (see Figure 4-23). The relative depth of each sample location is dependent on the oil volume. To permit visualization, less than 5L of oil was used during tests at speeds less than 4000rpm. Unless otherwise noted, 5L of oil was used during all experiments described in and after Section 4.3.

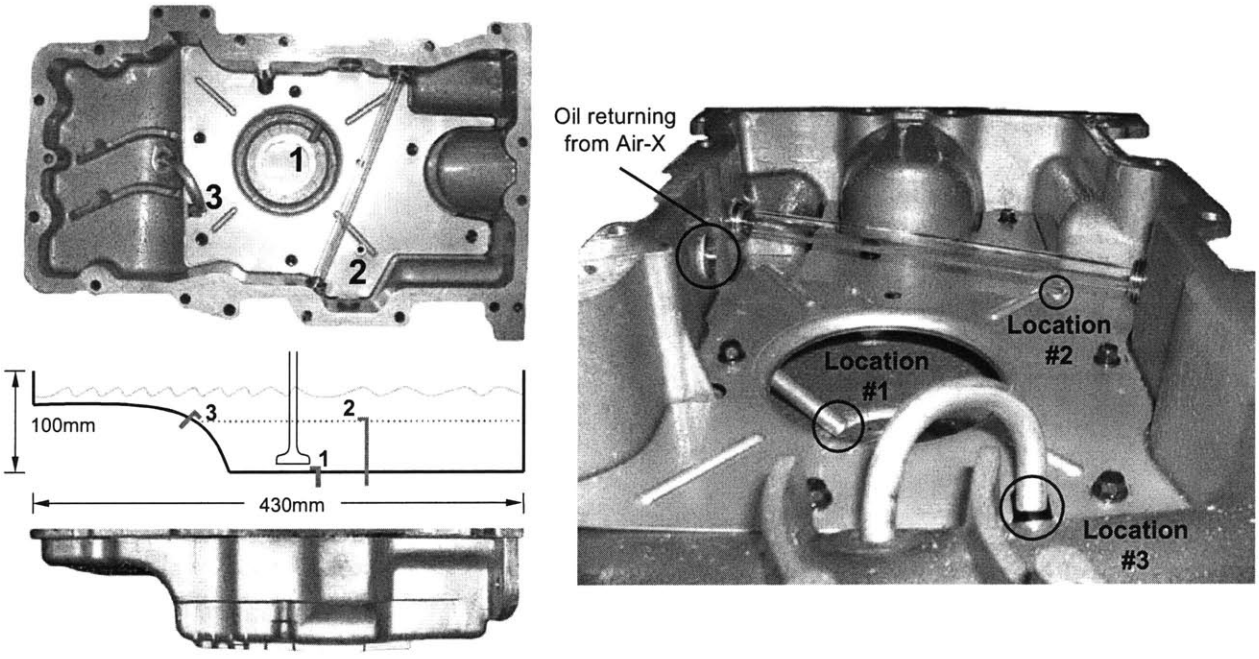

Figure 4-23. Oil pan Air-x sample locations. The approximate oil level is shown during experiments with 5L of engine oil.

4.3.1 Measurement Certainty

Cycling between the three sampling locations an experiment was performed over a range of near equilibrium temperatures between 80 and 105°C and engine speeds between 2000 and 6000rpm.

An equilibrium motoring oil temperature was achieved between 80 and 105°C at 2000rpm with no cooling water. Cooling water was required to keep the oil temperature within this range at the higher engine speeds (greater than 4000rpm). Eighty measurements were performed at each engine speed (20 measurements were required to obtain an equilibrium level of aeration and 20 measurements were taken at each of the three sample locations). The first three measurements at each location were neglected and the remaining 17 measurements were averaged. Typically, these 17 measurements varied by less than +/- 1.0% (see Figure 4-24).

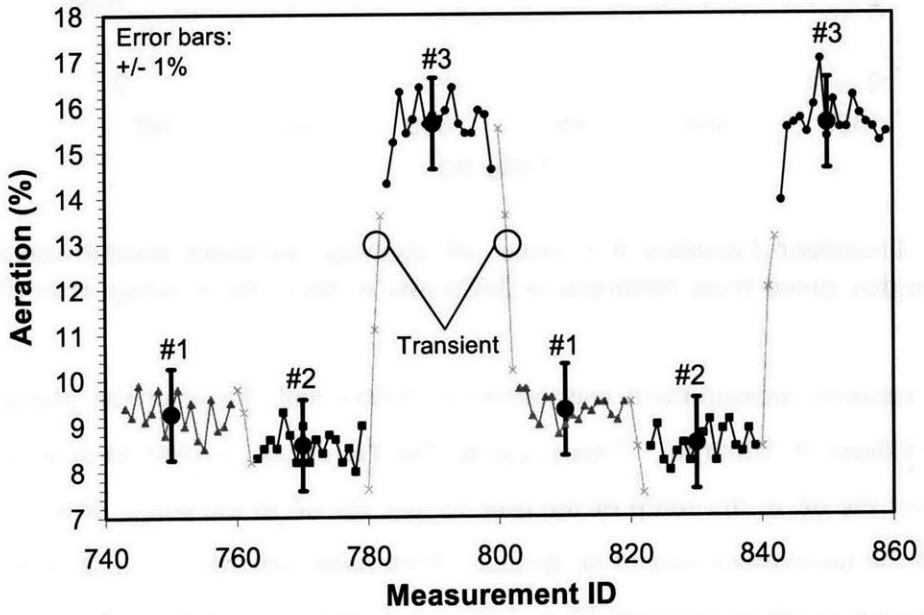

Figure 4-24. Typical aeration data at 3000rpm, with no windage tray. When the sampling location was cycled from one location to another, the first three data points were neglected and the following seventeen measurements were averaged. Location # 1 (near oil pick-up), Location # 2 (near head oil return), and Location # 3 (near oil surface). An error bar of +/- 1% is shown to highlight the repeatability of consecutive measurements.

4.3.2 Transient Aeration

During an increase or decrease in engine speed, typically 20 measurements (100s) were required for the aeration to reach a steady state. Shown in Figure 4-25 are transient aeration data during a decrease in engine speed from 5000rpm to 2000rpm.

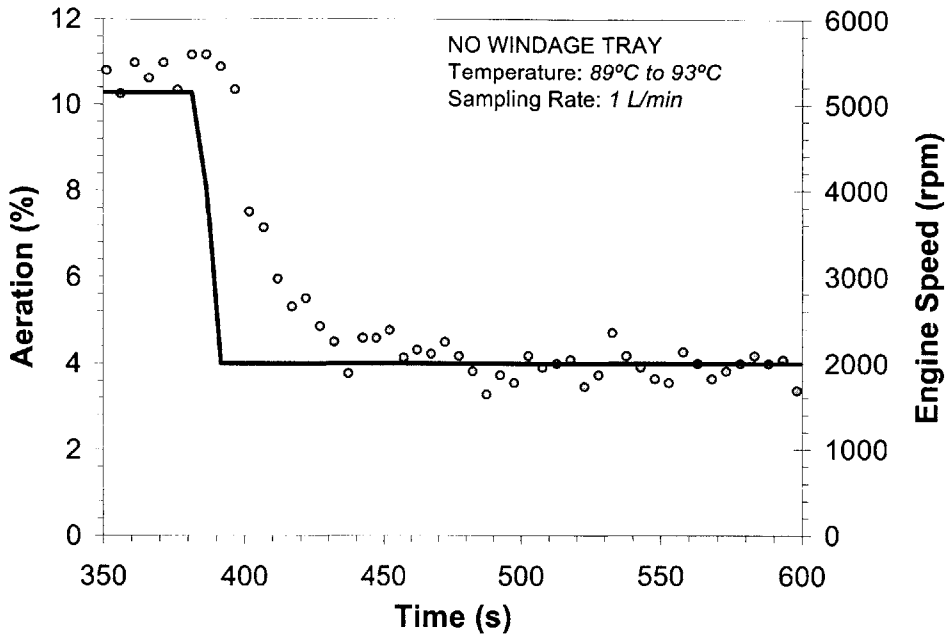

Figure 4-25. Transient Location # 1 (near oil pick-up) aeration measurement during a decrease in engine speed from 5000rpm to 2000rpm, without the windage tray (5L of oil).

A repeatable aeration measurement was observed before and 50s after the change in engine speed from 5000rpm to 2000rpm. This suggests that the decay in aeration is governed by the time to turnover the oil in the sump or the time to mix the oil in the sump, or a combination of both. Though the mechanism cannot be deduced from these experiments, Figure 4-25 indicates that it is necessary to allow between 10 and 20 measurements (50s and 100s) before a steady aeration measurement is achieved. Note that this was performed at near equilibrium oil temperatures.

4.3.3 Sampling Order

The sampling order was typically cycled between Location # 1 (near oil pick-up), Location # 2 (near head oil return), and Location # 3 (near oil surface), in that order. It was thought that the oil returning from Air-x may have an influence on the aeration measurement (see Figure 4-23 for geometry), and if the sampling order was always the same, this influence may never be observed. To assess this, an experiment from 2000rpm to 6000rpm was performed, randomly altering the sampling order of the measurement locations. The results of this experiment are shown for 4000rpm in Figure 4-26.

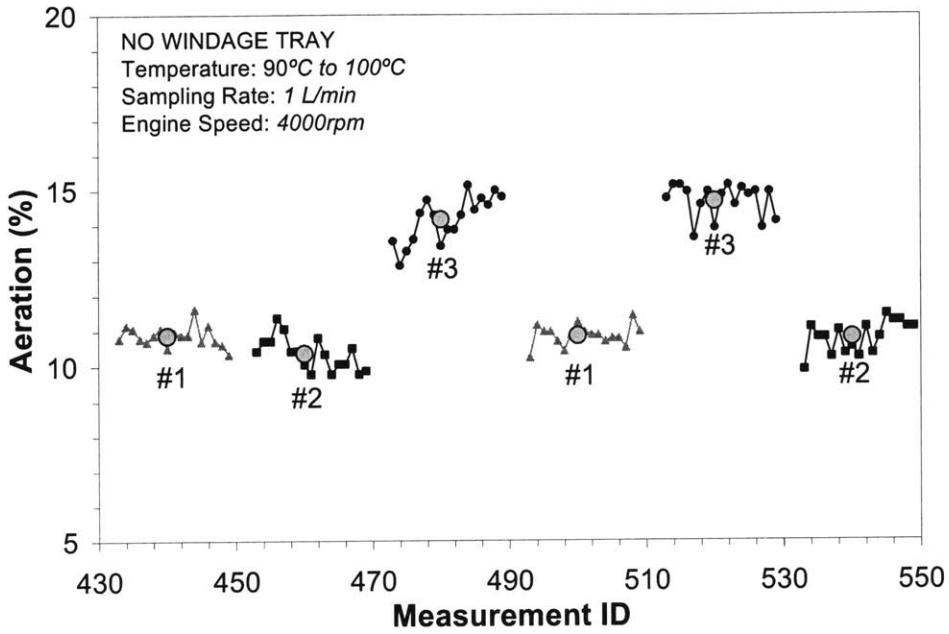

Figure 4-26. The sensitivity of aeration to the order of sampling at each location. The data are shown for a 4000rpm experiment performed without the windage tray. Location # 1 (near oil pick-up), Location # 2 (near head oil return), and Location # 3 (near oil surface). Each measurement ID is five seconds.

Based on the experiments performed between 2000rpm and 6000rpm, the aeration measurement is unaffected by the sampling order.

4.4 Experimental Results

4.4.1 The effect of engine speed

Twenty aeration measurements (5s per measurement) were performed at each location, neglecting the first three measurements at each location. In Figure 4-27, four averaged data points are shown at each engine speed and location. The baseline experiment was performed, which measured aeration at 2000rpm increasing to 6000rpm in 1000rpm increments. The second experiment was performed, which measured aeration at 2000rpm, followed by 5000rpm, 3000rpm, 6000rpm, and then 4000rpm. The third experiment was performed following the engine being shutdown for 100s after the second experiment. This gave the oil a chance to

partially de-aerate, while only moderately reducing its bulk temperature. The fourth experiment was performed 24h after the third experiment. By this time, the oil had completely de-aerated and cooled to room temperature. The data was processed similarly for all experiments and are shown in Figure 4-27.

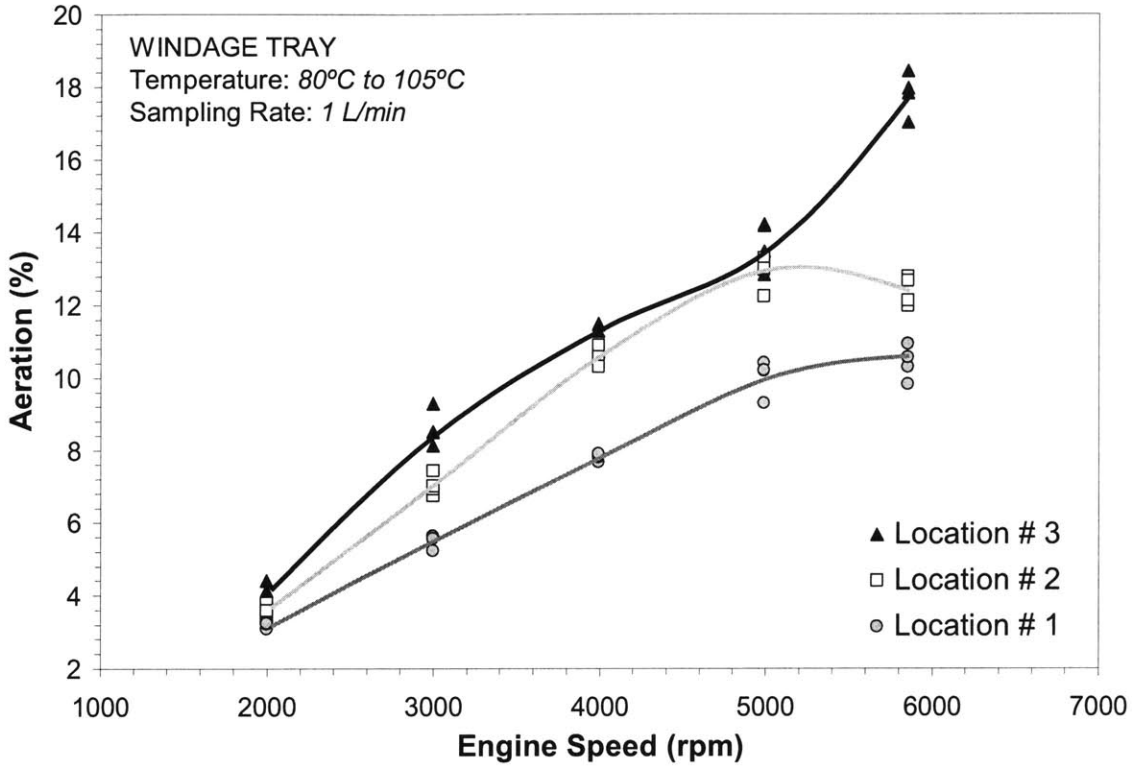

Figure 4-27. Four aeration experiments: Oil volume of 5quarts, windage tray, oil temperature between 80 and 105°C. Each of the four data points, at each of the sample locations and engine speed, represent one of the four experiments.

The aeration measurements were repeatable within +/- 1% for the same oil, oil volume, and operating temperature range (80 to 105°C). From this information, some general observations can be made. The near surface aeration (Location # 3) is greater than the near pick-up aeration (Location # 1) over the entire range of engine speeds examined. This indicates that the surface of the oil is more aerated than the oil entering the pick-up. This may be a result of the air bubbles rising to the surface due to gravity. As the engine speed increases, the aeration increases. This suggests that during an increase in engine speed, air may not be able to escape the oil fast enough. Alternatively, this may indicate that an aeration mechanism increases with

engine speed. During a decrease in engine speed, the oil is de-gassed. As the engine speed increases, the near surface aeration (Location # 3) and near oil pick-up aeration (Location # 1) follow the same increasing trend. This suggests that the oil aeration at the surface is related to the aeration at the pick-up. As the engine speed increases, the oil sump resident time decreases and less air can escape as compared to the low engine speed, higher oil sump resident time, condition. Beyond 5000rpm, the difference between the near surface (Location # 3) and the near pick-up (Location # 1) aeration increases. Though the oil sump resident time decreases as the engine speed increases, the sharp increase in aeration at the near oil surface (Location # 3) suggests that beyond 5000rpm either an additional aeration mechanism exists or significant oil surface sloshing is causing free air to enter the sampling tube. The near head oil return aeration (Location # 2) curve is situated between Locations # 1 and # 3. Though four experiments reveal a repeatable aeration measurement at Location # 2, it is difficult to determine the quantity of sampled oil that came from the head, thus making it difficult to draw any conclusions from the Location # 2 measurement.

4.4.2 The effect of the windage tray

A similar experiment was performed without the windage tray. An experiment was performed at 2000rpm, increasing in 1000rpm increments to 6000rpm. Twenty aeration measurements (5s per measurement) were performed at each location, neglecting the first three measurements at each location. After completing the experiment, the oil was cooled to room temperature and removed from the engine. Forty-eight hours later the oil was poured back into the sump and a second experiment was performed. Following the same procedure as the first experiment, a second set of data was obtained. Both of these experiments, without the windage tray, are shown in Figure 4-28.

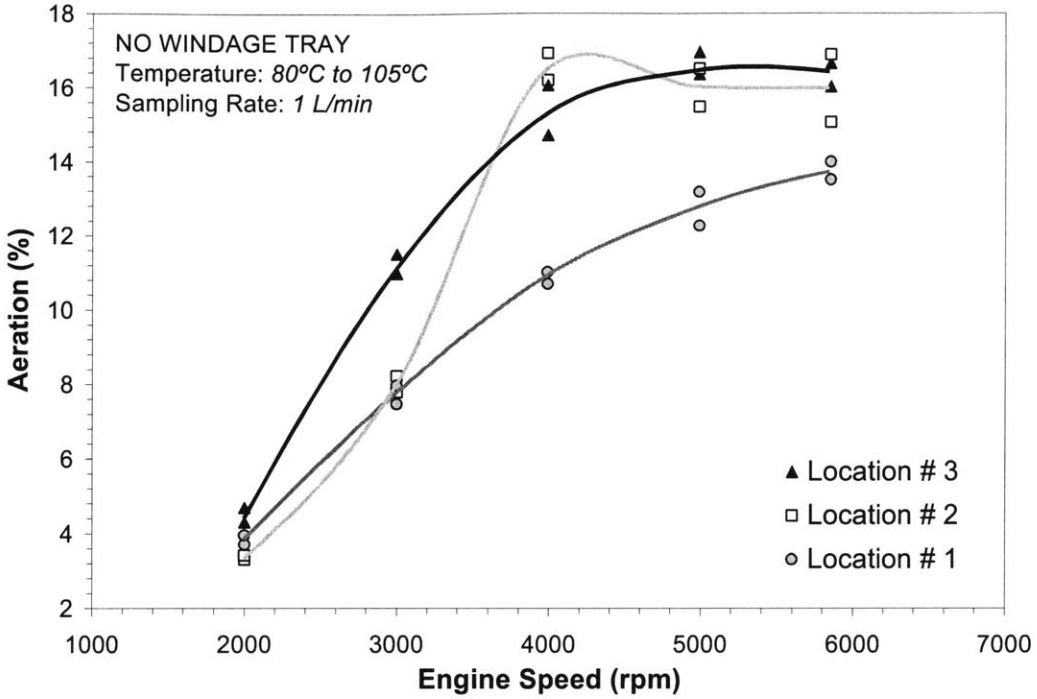

Figure 4-28. Two aeration experiments: Oil volume of 5L, no windage tray, oil temperature between 80 and 105°C. Each data point at a single sample location represents one of the two experiments performed. Location # 1 (near oil pick-up), Location # 2 (near head return oil), and Location # 3 (near oil surface).

Similar observations as the experiment with the windage tray can be made. Location # 3 (near oil surface) is more aerated than Location # 1 (near oil pick-up) over the entire range of engine speeds examined. This indicates that the surface of the oil is more aerated than the oil entering the pick-up. As the engine speed increases, the aeration increases. Since Location # 3 (near oil surface) and Location # 1 (near oil pick-up) follow the same trend, this suggests that the oil aeration at the surface is related to the aeration at the pick-up. The aeration at Location # 1 and Location # 3 are shown in Figure 4-29 for both the experiments with and without the windage tray.

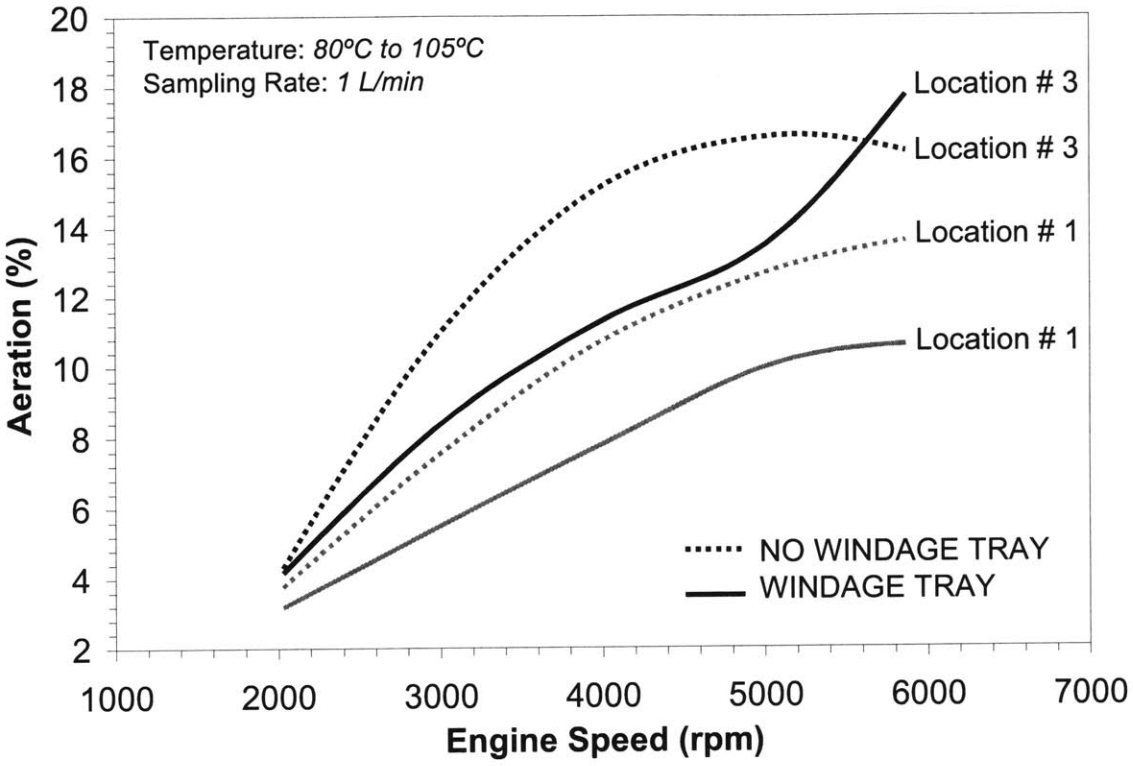

Figure 4-29. Aeration at Location # 1 (near oil pick-up) and Location #3 (near oil surface) for experiments with and without the windage tray.

Though the pick-up (Location # 1) and surface (Location # 3) aeration for both experiments (with and without the windage tray) follow the same trend below 5000rpm, a much different situation exists above 5000rpm. Above 5000rpm, the droplets departing the crankshaft are able to strike the oil surface with significant velocity, when no windage tray is present, and increase mixing in the sump. This phenomenon would likely result in the difference between the near surface (Location # 3) and near pick-up (Location # 1) aeration to decrease. Above 5000rpm, when the windage tray was present, there was a sharp increase in surface aeration, and the difference in aeration between the oil pick-up and surface increased. This suggests that above 5000rpm either an additional aeration mechanism exists or significant oil surface sloshing is causing the free air to enter the near oil surface (Location # 3) sampling tube.

4.4.3 The effect of oil sump resident time

The oil sump resident time is defined as the length of time to completely turn over the entire volume of oil in the sump. As the oil volume increases, the oil sump resident time increases. As the engine speed increases, the oil flow rate increases, thus decreasing the oil sump resident time.

Experiments were performed at 2000, 3000, and 4000rpm using oil volumes of 4, 4.5, and 5 quarts. Below 4000rpm, the aeration at Location # 1 (near oil pick-up) is more dependent on the engine speed than on oil volumes between 4 and 5L (see Figure 4-30).

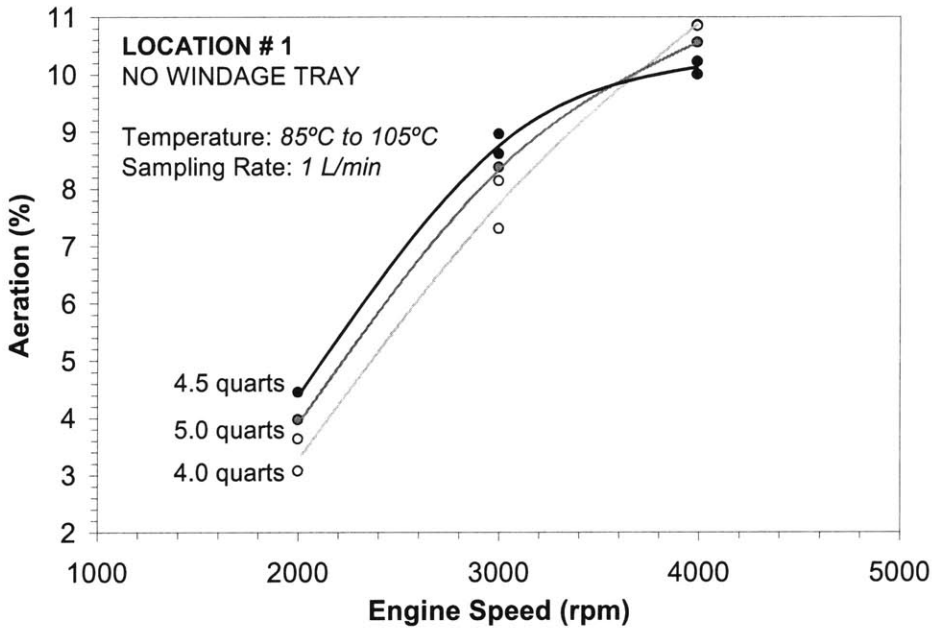

Figure 4-30. The effect of oil volume on aeration near the oil pick-up (Location # 1) without the windage tray.

Since the oil sump resident time decreases when the engine speed increases and the oil volume decreases, decoupling the engine speed and oil volume may reveal a general aeration trend. The oil sump resident time as a function of engine speed is shown in Figure 4-31.

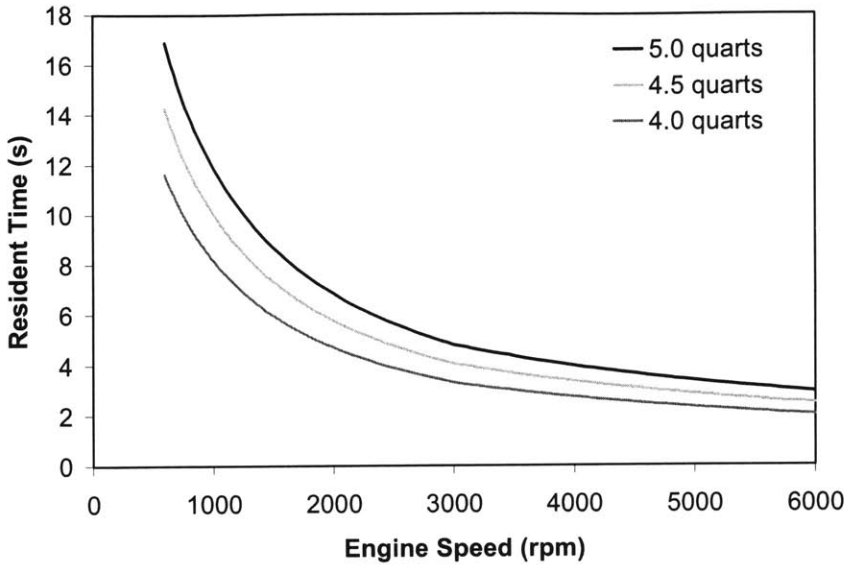

Figure 4-31. Oil sump resident time as a function of engine speed [2]

Since the engine speed has a greater affect on aeration than oil volume, this may suggest that, for the speed range considered in this experiment, identifying the aeration mechanisms and developing solutions will better serve to decrease aeration at the oil pick-up.

(This page is intentionally blank)

Chapter 5: Summary and Conclusions

5.1 Visual Observations

All visual observations were performed with between 4 and 4.5L of Motorcraft 5W20 in the sump. Many of the visual observations were performed below the firing engine oil temperature.

1. **OIL DROPLETS:** A high-speed droplet stream was flung from rotating crankshaft at near the tangential velocity. This stream passed through the drainage gap in the windage tray and struck the free surface of the oil in the sump, thereby agitating it. The droplet velocity and number density increased with engine speed.
2. **FOAM:** Foam was observed to form above a threshold engine speed and dissipated below a threshold engine speed. Foam formation was also dependent on the oil temperature. As the oil temperature increased (at a constant engine speed) foam formation was observed at a threshold oil temperature.
3. **WINDAGE TRAY:** The windage tray reduced the number of droplets entering the sump. No foam formation was observed when the windage tray was removed. This suggests that perhaps the droplets destroy foam on the surface of the oil.
4. **ENGINE LOAD:** In the oil sump, there was no visual difference between firing and motoring engine operation. No visual aeration difference was observed when the engine load varied from full load to part load.
5. **ENGINE SHUTDOWN:** During de-aeration (after the engine has been shut down), larger bubbles reached the surface faster than smaller bubbles, leaving the oil aerated with mostly smaller air bubbles.
6. **OIL SURFACE:** The oil surface sloshed at the same frequency as the crankshaft rotation. This suggests that a rhythmic pulsation of oil droplets enter the sump from above the windage tray, strike the surface of the oil, and cause the oil surface to slosh at a frequency proportional to engine speed.

The above observations suggested that foam formation was the net result of the competing air bubble creation and destruction processes. The rates of these processes were speed dependent; hence there was a speed threshold for foam formation.

5.2 On-line Oil Aeration Measurements

Aeration is dependent on many parameters, including the engine speed, oil temperature and pressure, oil volume, and sump design. A method of measuring oil aeration in the sump was developed, though the difficulty in measuring the head oil return aeration reveals the complexities of quantifying aeration. Based on preliminary Air-x aeration measurements in three locations around the oil sump, the following conclusions were made:

1. The surface was always more aerated than the pick-up.
2. As the engine speed increased to 5000rpm the oil aeration increased at both the surface and pick-up. Since they increased at similar rates it suggests that the air cannot de-aerate because of the decreased oil sump residence time associated with an increase in engine speed.
3. As the engine speed increased to 5000rpm, the aeration at both the pick-up and surface was greater without the windage tray as compared to with the windage tray. This suggests that below 5000rpm the windage tray decreases oil aeration.
4. With the windage tray, the difference in aeration between the surface of the oil and near the pick-up increased above 5000rpm. This suggests that above 5000rpm perhaps a critical aeration creation mechanism exists or free air is being drawn into the oil surface sampling tube.
5. Without the windage tray, the difference in aeration between the surface of the oil and near the pick-up decreased above 5000rpm. Perhaps the surface agitation caused by unshielded droplets striking the oil surface enhanced oil mixing and decreased the difference in aeration between the surface and pick-up. Alternatively, the increased droplet number density may cause surface agitation, resulting in air being drawn into the sampling tube.

5.3 General Conclusions

Along the oil's journey through the oil lube system, the oil lubricates, cools, removes impurities, supports load, and minimizes friction. At the end of the oil's journey it returns to the sump where it remains nearly motionless until it re-enters the oil pick-up and restarts its journey. As the oil sits in the sump, oil droplets departing the crankshaft continuously pelt the free surface of

the oil, causing the surface to rhythmically pulsate at the frequency of the crankshaft. As the engine speed increases, more droplets strike the surface, however the windage tray reduces the number of droplets and ensures that the oil remains in the sump and does not come into contact with the crankshaft. At a specific engine speed and oil temperature, air bubbles located below the oil surface, break the surface and form a foam network that is only broken when the engine speed or temperature fall below a threshold or when droplets are able to strike the foam.

In the oil sump, more air is present at the oil surface than at the oil pick-up because air continuously leaves the oil at the air-oil interface. As the engine speed increases, less air is able to leave the oil before the oil restarts its journey through the lube system because the resident time is reduced. Air continuously enters the oil, but because of the many oil re-entry locations, the difficulties in measuring the aeration at the re-entry location, and the inability to measure the oil flow from each re-entry location it is difficult to determine where the air enters the oil.

When the engine shuts down, all of the oil on its journey through the lube system drains back into the oil sump, and the air bubbles escape the oil.

5.4 Future Work

Though a visual experiment was performed in the oil sump region and preliminary Air-x measurements were used to observe some general aeration features, further experimentation and analysis would significantly add to this current study.

1. **FOAM FORMATION:** Foam formation was observed visually in the oil sump, though no aeration measurements were performed in the known presence of foam. Visualization in the oil sump during aeration measurements may answer this question. Further investigations into the formation of foam and its influence on the oil sump aeration would be beneficial.

2. **FIRING ENGINE OPERATION:** On a firing engine, gas blowby and the increased combustion load on bearings may influence sump aeration. Visualization experiments

were performed on a firing engine and extending that study to Air-x measurements would be beneficial.

3. **AIR-X MEASUREMENTS:** Air-x measurements were performed only in the oil sump. Extending this study to other regions of the lube path would enhance the understanding of the aeration creation and destruction mechanisms. For example, further engine modifications to allow for measurements in the main gallery, near the timing chain, and in the heads may assist in determining the aeration source.

4. **MODELING AERATION:** A computational fluid dynamics model of the oil sump would establish air transport mechanisms from the oil sump entry locations to the oil pick-up. In conjunction with aeration measurements in three sump locations, the head gallery, and the main gallery, the aeration creation and destruction mechanisms could be elucidated.

5. **WINDAGE TRAY:** The windage tray function is unclear even to oil lube designers. The windage tray stops oil from sloshing and coming into contact with the crankshaft. The windage tray also scrapes oil off of the crankshaft and shields the oil sump from high-speed droplets. Perhaps the oil that collects on the windage tray, before entering sump, is able to partially de-aerate. If the oil atop the windage tray comes into contact with the crankshaft and imparts a drag load on the crankshaft, this may increase aeration. There would be great value in better understanding the function of the windage tray. By redesigning the windage tray, this could be experimentally studied.

6. **ENGINE OIL:** Oil additives have been shown to reduce aeration, though an experimental study has not been performed. Aging the oil and changing the oil weight and composition may also affect aeration. Preliminary experiments into varying the oil volume were performed, but further investigation into all of these effects would greatly benefit the development of a complete engine oil aeration study.

References

1. Heywood, J., Internal Combustion Engine Fundamentals. 1988, New York: McGraw-Hill.

2. Ni, B., E-mail Communication, November 1, 2004, Boston.

3. Totten, G., Sun, Y., and Bishop, R. "Hydraulic Fluids: Foaming, Air Entrainment and Air Release - A Review," SAE 972789, 1997.

4. Magorien, V. "How Hydraulic Fluids Generate Air," Hydraulics & Pneumatics, 1968: p. 104-108.

5. Koch, F., Hardt, T., and Haubner, F. "Oil Aeration in Combustion Engine - Analysis and Optimization," SAE 2001-01-1074, 2001.

6. Haas, A., Geiger, U., and Maaben, F. "Oil Aeration in High Speed Combustion Engines," SAE 940792, 1994.

7. Nemoto, S., Kawata, K., Kuribayashi, T., Akiyama, K., Kawai, H., and Murakawa, H. "A study of engine oil aeration," JSAE Review, 1997. **18**: p. 271-276.

8. Olander, K., and Mayr, B. "Design and Special Development Problems of Mercedes-Benz V-8 Engines," SAE 750051, 1975.

9. Maassen, F., Koch, F., and Pischinger, F. "Connecting Rod Bearing Operation with Aerated Lube Oil," SAE 981404, 1998.

10. Yano, H., and Yabumoto, J. "The Behavior of Entrained Gas Bubbles in Engine Oil and the Development of Effective Gas-Oil Separators," SAE 900812, 1990.

11. Brégent, R., Porot, P., Monchaux, E., and Cailliez, J. "The SMAC, under Pressure Oil Aeration Measurement System in Running Engines," SAE 2000-01-1818, 2000.

12. Deconninck, B., Delvigne, T., and Videx, G. "Air-X, an Innovative Device for On-Line Oil Aeration Measurement in Running Engines," SAE 2003-01-1995, 2003.

13. Duncanson, M. "Effects of Physical and Chemical Properties on Foam in Lubricating Oils," J. Society of Tribologists and Lubrication Engineers, 2003. **59**: p. 9-13.

14. Reid, R., Prausnitz, J., and Sherwood, T., The Properties of Gases and Liquids. 1977: McGraw Hill.

15. Chun, S., Park, Y., and Jang, S. "A Study on Engine Lubrication System by Optimized Network Analysis - Part II: Parametric Study," SAE 2000-01-2923, 2000.

16. Ni, B., and Pieprzak, J. "Transportation and Transformation of Air Bubbles in Aerated Oil through an Engine Lubrication System," SAE 2004-01-2915, 2004.

17. Stepina, V., and Vesely, V., Lubricants and Special Fluids. Tribology Series. Vol. 23. 1992, New York: Elsevier.

18. Weaire, D., and Hutzler, S., The Physics of Foams. 1999, Oxford: Clarendon Press.

19. Manz, D., Cowart, J., and Cheng, W. "High-speed Video Observation of Engine Oil Aeration," SAE 2004-01-2913, 2004.

20. Garrett, P., Defoaming. Theory and Industrial Application. 1993, New York: Marcel Dekker, Inc.

21. Nikolajsen, J. "The Effect of Aerated Oil on the Load Capacity of a Plain Journal Bearing," Tribology Transactions, 1999. **42**: p. 58-62.

22. Hayward, A., "The Viscosity of Bubble Oil", 1961, National Engineering Laboratory, Fluids Report No. 99.

23. Chun, S. "A parametric study on bubbly lubrication of high-speed journal bearings," Tribology International, 2002. **35**: p. 1-13.

24. Choi, J., Min, B., and Han, D. "Effect of Oil Aeration Rate on the Minimum Oil Film Thickness and Reliability of Engine Bearing," SAE 932785, 1993.

25. Porot, P., and Trapy, J. "A Numerical and Experimental Study of the Effect of Aeration of Oil on Valve Trains Equipped with Hydraulic Lash Adjusters," SAE 930997, 1993.

26. Zhao, Y., Tong, K., and Lu, J. "Determination of Aeration of Oil in High Pressure Chamber of Hydraulic Lash Adjuster in Valve Train," SAE 1999-01-0646, 1999.

27. Morgan, C., Cummings, J., Fewkes, R., and Mathew Jackson, J. "A New Method of Measuring Aeration and Deaeration of Fluids," SAE 2004-01-2914, 2004.